Althunibat et al., 2024
J. Basic Appl. Res biomed 10(1): 64-79

10.51152/jbarbiomed.v10i1.241

JBAAR
Journal of Basic and Applied Research in Biomedicine
ISSN 2413-7014

Original Article

Three Novel Triterpene Glycosides from the Sea Cucumber *Stichopus chloronotus* with Potent Cytotoxic Activities

Osama Y. Althunibat[1], Ridzwan Bin Hashim[2], Muhammad Taher[3], Jamaludin Mohd. Daud[4]

[1]Department of Medical Analysis, Princess Aisha Bint Al-Hussein Faculty of Nursing and Health Sciences, Al-Hussein Bin Talal University, Ma'an, 71111, Jordan.
[2]Faculty of Allied Health Sciences, International Islamic University Malaysia, Kuantan, Pahang 25200, Malaysia
[3]Faculty of Pharmacy, International Islamic University Malaysia, Jalan Sultan Ahmad Shah, Kuantan, Pahang 25200, Malaysia
[4]Faculty of Science, International Islamic University Malaysia, Jalan Istana Bandar Indera Mahkota, 25200, Kuantan, Pahang, Malaysia

*Corresponding Author: thnibatjust2001@yahoo.com

Received: 15-11-2024
Revised: 20-12-2024
Published: 19-12-2024

Keywords:
Stichopus chloronotus,
Triterpene Glycosides,
Sea Cucumber,
Cytotoxicity

Abstract: This study aimed to isolate the active cytotoxic compounds from *Stichopus chloronotus*. The isolation process was carried out by using successive separation methods including liquid-liquid partitioning, vacuum liquid chromatography (VLC), size exclusion chromatography, normal and reverse phase chromatography, and HPLC which had been guided by the cytotoxic assay (MTT). The bioassay guided separation technique led to isolation of three new cytotoxic saponins (A, B, and C), which exhibited positive reactions with Liebermann–Burchard reagent. The structures of the isolated compounds were elucidated based on the interpretation of their spectra upon analyzing them with various spectroscopic methods including infra-red spectrophotometry (IR), one and two dimensional nuclear magnetic resonance (NMR), in addition to the positive mode of electrospray mass analysis (+ESI-MS). Based on the analysis, the structures of the isolated compounds were concluded as triterpene glycosides composed of holostane type aglycones attached to various sulphated sugar units. The molecular formula of the glycoside A was suggested as C_{66} $H_{104}Na_2O_{36}S_2$ (calculated molecular weight = 1583.62 Da), B as $C_{66}H_{103}Na_3O_{40}S_3$ (MW= 1701.66 Da) and glycoside C as $C_{66}H_{100}Na_4O_{43}S_4$ (MW= 1801.69 Da). Furthermore, the cytotoxic effects of the isolated glycosides (A, B, and C) were evaluated against various cancer cell lines and found that the glycoside C (IC_{50} = 0.9-2.4 µM) was the most potent cytotoxic glycoside, followed by glycoside B (IC_{50} = 1.3-2.9 µM) and A (IC_{50} = 2.4-7.5 µM). These findings, therefore, present *S. chloronotus* as a promising source of novel cytotoxic saponins with potent anti-cancer activities that require further research into their modes of action and therapeutic applications.

Cite this article as: Althunibat, O., Hashim, R., Taher, M., Daud, J.M. (2024) Three Novel Triterpene Glycosides from the Sea Cucumber *Stichopus chloronotus* with Potent Cytotoxic Activities. Journal of Basic and Applied Research in Biomedicine, 10(1): 64-79. 10.51152/jbarbiomed.v10i1.241

INTRODUCTION

Stichopus chloronotus (Greenfish) is a sea cucumber species belongs to Stichopodidae family, Aspidochirotida order and Aspidochirotacea subclass. *S. chloronotus* is a deep black-green sea cucumber with a firm body of quadrangular shape containing yellow/ red tips to the papillae. The ventral mouth is surrounded by a row of 20 stout tentacles, and its body covered with a smooth green tegument that gives it the name of greenfish (CONAND et al., 2002; Uthicke et al., 2001). *S. chloronotus* is distributed throughout the tropical Indo-Pacific region, and it has been found in different Malaysian coastal areas including Peninsular Malaysia as well as East Malaysia. It can be found in shallow areas on the fine sand and among living coral and algae habitat (Ridzwan, 2007; Solehin et al., 2021).

S. chloronotus is one of the high value species which are dried and internationally traded in a product called "*Trepang*" or "*Bech-de-mer*". Furthermore, *Stichopus* genus (*gamat*) has been used in traditional medicine since ancient time. It is taken to cure various diseases such as pneumonia, joint aches and deep wounds (Ridzwan, 2007). On the other sites, crude extracts of *S. chloronotus* have exhibited various biological and pharmaceutical properties in scientific experiments (Li et al., 2024; Yin et al., 2024). Antinociceptive activities of several aqueous and organic extracts have been demonstrated in mice by using the abdominal contraction and hot tail-flick test (Maskur et al., 2024; Ridzwan et al., 2001). *S. chloronotus* extracts possessed antifungal activities against different pathogenic fungi by using *in vitro* and *in vivo* models, without causing any side effect or allergic reaction on the treated skin (Hing et al., 2007; Mazlan et al., 2023). The wound healing effect of *S. chloronotus* was verified by the study conducted by Fredalina and colleagues (Fredalina et al., 1999). Although *S. chloronotus* has shown various promising pharmaceutical and biological effects, only few studies have been conducted to identify the active components of this species. Three ganglioside molecular species, SCG-1, SCG-2, and SCG-3, were isolated from the lipid fraction of *S. chloronotus*, and they exhibited neuritogenic activities toward the rat pheochromocytoma PC12 cells (Yamada et al., 2003). Fatty acid profile from crude extracts of *S. chloronotus* was determined using gas chromatography (GC) technique. It is believed that the isolated fatty acids including arachidonic acid (AA C20:4), eicosapentaenoic acid (EPA C20:5), and docosahexaenoic acid (DHA C22:6) play a potential role in tissue repair and wound healing effects of *S. chloronotus* (Fredalina et al., 1999). In earlier study, six antifungal triterpene oligoglycosides were isolated from *S. chloronotus* extract (Kitagawa, Kobayashi, Inamoto, Yasuzawa, & Kyogoku, 1981). Yin et al., demonstrated that fucosylated chondroitin sulfate (fCS-Sc), isolated from S. *chloronotus*, improves intestinal barrier integrity, antioxidant defenses, and gut microbiota balance, alleviating Cyclophosphamide-induced damage (Yin et al., 2024). In general, the therapeutic properties and medicinal benefits of sea cucumber species are ascribed to the presence of a variety of bioactive compounds such as triterpene glycosides (saponins), chondroitin sulphates, glycosaminoglycan (GAGs), sulphated polysaccharides, sterols (glycosides and sulphates), phenolics, cerberosides, lectins, peptides, glycoprotein, glycosphingolipids and essential fatty acids. Employment of modern chromatographic and isolation techniques has resulted in isolation several novel bioactive compounds from various sea cucumber species. Many of these isolated compounds have exhibited unique biological and pharmaceutical activities such

as anti-angiogenic (philinopside E and A), anticoagulant (fucosylated chondroitin sulphate), anti-hypertension (peptide), antifungal (holothurin B and A), antioxidant (peptide), antithrombotic (sulphated polysaccharide), antiviral (liouvillosides A and B) and wound healing (arachidonic acid) (Bordbar et al., 2011; Hossain et al., 2023; Mohd Heikal et al., 2019; Mohd Yunus et al., 2019).

Moreover, a number of studies have isolated several compounds with potential cytotoxic effects against various cancer cells. Spectroscopic analysis of the isolated anticancer compounds demonstrated their diverse chemical structures. However, most of the identified cytotoxic compounds were found to be triterpene glycosides (saponins). Three triterpene glycosides, intercedensides A, B and C isolated from the sea cucumber, *Mensamaria intercedens*, exhibited potent cytotoxic activities against human tumour cell lines (Zou et al., 2003). In addition, Silchenko et al. (2008) isolated three new triterpene oligoglycosides, okhotosides B1, B2 and B3, along with the known compounds frondoside A, cucumarioside A2-5 and koreoside A from sea cucumber *Cucumaria okhotensis*. The isolated glycosides demonstrated various levels of cytotoxic effects against THP-1 and HeLa tumour cell lines (Silchenko et al., 2008). Furthermore, two new triterpene glycosides, scabraside A and B which were isolated from *H. scabra*, showed potent cytotoxic activities against multiple tumour cell lines (Han et al., 2012). Stichoposide D, a triterpene saponin from *S. chloronotus*, demonstrated strong cytotoxic activity against leukemias and potential anti-cancer stem cell (CSC) activity in pluripotent human embryonic carcinoma NTERA-2 cells (Cuc et al., 2020).

On the other hand, the hydrophobic sphingoid bases, isolated from *Stichopus variegate* cerberosides, showed strong cytotoxic activity against cancer cells, DLD-1, WiDr and Caco-2 cells (SUGAWARA et al., 2006). Yang et al. (2003) isolated a branched-chain fatty acid, 12-methyltetradecanoic acid, from sea cucumber extract and demonstrated its antiproliferative effect against prostate cancer cells (PC3) (P. Yang et al., 2003). In addition, myristoleic acid, isolated from the oil of the sea cucumber *C. frondosa*, showed antitumour activities by using *in vitro* and *in vivo* models (Ding et al., 2004). Eight sulfated triterpene glycosides were isolated from *Psolus peronii*, including peronioside A and psolusosides A, B, G, I, L, N, and P. Among these, psolusosides A and L showed the strongest cytotoxic activity against breast cancer cell lines MCF-7, T-47D, and MDA-MB-231 (Silchenko et al., 2024).

In the previous investigation, *S. chloronotus* extracts showed the most potential cytotoxic effects among the tested sea cucumber species (Althunibat et al., 2009). Despite the great number of cytotoxic compounds that have been isolated from different species of sea cucumber, to the best of our knowledge, no study has been carried out to isolate and identify the cytotoxic compounds from *S. chloronotus*. Hence, this study was aimed to isolate the active cytotoxic compounds from *S. chloronotus* by using a bioassay guided isolation technique.

MATERIAL AND METHODS

Biological Assay

MTT Assay

The fractionation and isolation process of the active cytotoxic compounds from *S. chloronotus* extract had been guided by the results of MTT (3-(4,5- dimethylthiazol-2-yl)-2,5-diphenyltetrazolium bromide) assay. In brief, the cells were seeded in a complete medium in a 96-well plate ($1x10^4$ cells/well). After reaching confluent, the cells were incubated with different samples concentrations for 48 h. The vehicles (DMSO and PBS) were used as controls. The medium was then discarded and the adherent cells were washed with phosphate buffer saline (PBS). Then, 20 µl of MTT stock solution (5 mg/mL in PBS) were added to each well and the plates were further incubated overnight at 37 °C. Next, 100 µL of DMSO was added to each well to solubilize the formazan crystals produced by the viable cells. After complete dissolving of formazan blue, an absorbance was measured at 570 nm and a reference wavelength of 690 nm using Versa MaxTM Tunable microplate reader. The percentage of cell viability was calculated according to the equation described in Moongkarndi et al. (2004).

% Cell viability = (OD of treated cells / OD of control cells) × 100

The experiment was repeated three times and the mean values of extract concentrations required for inhibition of 50% of cell viability (IC_{50}) were determined.

Cell lines

Four human cancer cell lines; human non-small lung carcinoma (A549), human cervical cancer (C33A), human breast adenocarcinoma (MCF-7), human esophageal carcinoma (TE1) were used to evaluate the cytotoxic effects of the tested extracts. In addition to that, normal human fibroblast (NHDF) cell line was used in this study. All the cell lines were kindly provided by Dr. Masa-aki Ikeda; Department of Molecular and Craniofacial Embryology, Tokyo Medical and Dental University, through Dr. Solachuddin J. A. Ichwan, Kulliyyah of Dentistry, IIUM.

Human non-small lung carcinoma (A549) had been used in MTT assay to assay the cytotoxic compounds during the isolation process. Furthermore, after purification of the active compounds, their cytotoxic effect were verified against additional four cancer and normal cell lines including, human cervical cancer (C33A), human breast adenocarcinoma (MCF-7), human esophageal carcinoma (TE1) and normal human dermal fibroblasts (NHDF). All cell lines were cultured in Dulbecco`s modified Eagle medium (DMEM) containing 10% heat inactivated fetal bovine serum (FBS) and 1% penicillin-streptomycin. The cells were maintained in a humidified atmosphere provided with 5% CO_2 at 37°C.

Sample Collection and Extraction

S. chloronotus samples (3.0 kg) were collected from Terengganu costal area, Malaysia. The taxonomis identification of the species was carried out by Prof. Dr. Ridzwan Bin Hashim, according to the morphological and genetic study conducted by his research group (Kamarudin et al., 2010). Voucher specimens (Tg7) have been deposited at the museum in Faculty of Science, International Islamic University Malaysia. The sample was dissected to remove the internal organs, and packed immediately with ice prior sending to the laboratory to be kept at –80°C. The frozen sample was chopped into small pieces and then freeze dried in before it was extracted with a polar organic solvent, methanol. The methanolic extract was obtained by homogenizing a dried sample (350.0 g) two times with 5 L of methanol. The homogenized mixture had been stirred overnight before it was filtered through a Whatman filter paper No.4. The solvent was evaporated by rotary evaporator at 40 °C under vacuum yielding 41.0 g of crude methanolic extract. The methanolic extract was then assessed by MTT assay to verify its cytotoxic potential.

Liquid-Liquid Extraction

The crude methanolic extract of *S. chloronotus* was subjected into sequential gradient partitioning in order to separate its natural constituents according to their polarity (Riguera, 1998). First, the crude extract was partitioned between the same volume of hexane and a mixture of methanol-water (9:1) in a separatory funnel. The hydro-alcoholic fraction was further partitioned between carbon tetrachloride (CCl_4) and methanol-water mixture (8:2). Furthermore, the new obtained hydro-alcoholic fraction was partitioned again between a mixture of methanol-water (6:4) and dichloromethane (CH_2Cl_2). Finally, methanol was evaporated completely from the hydro alcoholic fraction and its natural compounds were partitioned between water and *n*-butanol (*n*-BuOH). Organic solvents were removed from the fractions by rotary evaporator at 40 °C, while the water fraction was freeze-dried. Yield of each fraction was calculated, and the cytotoxicity test (MTT assay) was performed to demonstrate the cytotoxic property of each fraction against the cancer cell line (A549 cells).

Desalting

The resin column was prepared according to the manufacturer instructions. First, Amberlite XAD-2 (200 g) was stirred and soaked in 500 mL beaker with methanol for 15 minutes. Subsequently, methanol was removed by decantation and replaced by distilled water. After 15 min, the resin slurry was poured into column (5cm x 1m). Excess water was drained from the bottom of the column, and then slow backward water flow was introduced from bottom to the top of the column. This was achieved by connecting the column bottom with deionized water container located at higher stage. The water flow rate was maintained until all air bubble and resin fines were dislodged from the bed suspension. Subsequently, the backward water flow was stopped to allow the resin particles to be arranged inside the column according to their sizes, in which the larger particles set at the bottom, while the smaller ones were settled at the top of the column. The water level was adjusted to be 2.5 cm above the top of the resin bed, and then 2.0 g of *n*-butanol fraction sample, dissolved in 20 mL water, was poured inside the column slowly at flow rate (2 mL/5 min) to allow the organic components to be adsorbed into the resin. After retention of the soluble organic compounds by Amberlite XAD-2 resin, the mineral salts were removed by water mobile phase. Subsequently, the adsorbed organic components were eluted from the resin by methanol. The process was repeated several times to yield 10.2 g of desalted fraction from the whole amount of n-butanole fraction (16.5 g).

Vacuum Liquid Chromatography (VLC)

The desalted organic compounds were further fractionated by vacuum liquid chromatography method. For this purpose, two aliquots of the desalted sample (5.1 g in each) were dissolved in 25 mL of MeOH:$CHCL_3$ (1:9) solvent. Sample was then chromatographed under vacuum system through a bed of silica gel (250 g, 230-400 Mesh ASTM, Merck) packed in sintered glass Buchner filter funnel of the VLC apparatus (8 cm diameter). Mobile phases of gradient increasing methanol concentration in MeOH-$CHCL_3$ mixture, started from 10% up to 100% MeOH, were used to elute ten subfractions. The obtained subfractions were labeled as BV10, BV20, BV30 up to BV100, in which B stood for butanol fraction; V stood for VLC method, while the numbers represented percentage of methanol in the mobile phases. The potent cytotoxic sub-fractions were identified by MTT assay, and then they were further subjected into thin layer chromatographic (TLC) technique in order to demonstrate their chemical compositions.

Thin Layer Chromatography (TLC)

The subfractions of BV4, BV5, BV6, BV7, BV8, BV9, and BV10 were found to have active compounds that exhibited significant cytotoxic effects against A549 in MTT assay. Thus, these subfractions were applied to TLC in order to observe their chemical profiles and to find a proper mobile phase that can isolate the active components. After testing several mobile phase systems on TLC plates (Silica Gel 60, Merck), the best separation profile was demonstrated by using a mobile phase composed of chloroform, methanol and water in a ratio of 8:2:0.1. The developed TLC plates were observed directly under visible, short UV (240 nm) and long UV (265 nm) lamps. In addition, they were visualized by iodine vapor which can react with the unsaturated bonds. Furthermore, TLC plates were visualized after heating at 110°C for 10 min with p-anisaldehyde–sulfuric acid reagent, which is sensitive to most functional groups such as terpenoids, propylpropanoids, and saponins. The reagent was prepared by adding 5 mL of concentrated sulfuric acid, 1.5 mL of glacial acetic acid and 3.7 mL of p-anisaldehyde to 135 mL of absolute ethanol (Waksmundzka-Hajnos et al., 2008).

Interestingly, all the active subfractions were found to have three major bands which could be observed by iodine vapour and p-anisaldehyde–sulfuric acid reagent but not directly under visible and UV lamps. Therefore, all the active subfractions, containing the three bands, were combined together (8.0 g) and labeled as "BVC" to be subjected into further isolation techniques

Size Exclusion Chromatography

Sephadex LH-20 polymer (GE Health care) was used as a bead medium for gel filtration of the cytotoxic active fraction (BVC). According to the manufacturer instructions, 30 g of Sephadex LH-20 powder were mixed with excess amount of methanol in 200 mL beaker, and stirred gently with glass rod. The bed slurry had been left overnight for complete swelling of the gel, and then it was resuspended and poured into the column (1.5 cm x 50 cm) in one continuous motion. The column was left to let the packing settled overnight, until the media bed has reached a constant height.

0.5 g of BVC fraction, dissolved in 5 mL of 20% $CHCl_3$ in MeOH, was applied into the packed Sephadex LH-20 column and eluted by methanol in a flow rate equal to 0.5 mL/min. The eluted fractions were collected into 1.5 mL fraction volume and they were tested on TLC to reveal their chemical components. The three major bands, which were visualized before in the active VLC fractions, were found to be eluted from Sephadex LH-20 column together and at the first collected fractions, indicating that their molecular sizes are close to each other and relatively larger than the other compounds in BVC fraction. These three compounds were labeled as A, B and C, according to their sequence on TLC plate from the top to the bottom, respectively. After repeating the Sephadex column elution several times, the eluted fractions that contained only compounds A, B and C were collected together and labeled as ABC fraction (4.5 g). Cytotoxic activity of ABC fraction was confirmed by MTT assay, and then it was subjected into further column chromatographic techniques in order to separate the three compounds from each other.

Normal Phase Column Chromatography

ABC fraction (2X 2.3 g) was dissolved in 10 mL of 60% $CHCl_3$ in MeOH, and subjected into column (5cm x 75 cm) packed with silica gel (150 g, 230-400 Mesh ASTM, Merck). A mobile phase composed of chloroform, methanol and water (8:2:0.1), was developed based on the TLC trials to be used for elution of the chromatographed compounds in a flow rate (1 ml/min) and fraction volume equal to 5 mL. Collected fractions were analyzed by TLC method using the same mobile phase, and then visualized by iodine vapour.

TLC results showed that normal phase chromatographic techniques was not the ideal method for purification of A, B and C compounds, since most of the collected fractions contained one major compound of A, B, and C in addition to some impurities of the subsequent or preceding compounds. Accordingly, three different fraction combinations were obtained from the normal silica column, labeled as Ab (0.9 g), aBc (1.1 g) and Cb (0.8 g), in which the capital letter represented the major compound in the fraction. Subsequently, the collected fractions were chromatographed using reverse phase TLC and column chromatographic techniques.

Reverse Phase Thin Layer Chromatography

Before applying the reverse phase column chromatographic technique to purify A, B, and C compounds, ABC fraction was analyzed on reverse phase thin layer chromatography by using C18 silica gel coated on aluminum sheet (Merck C18). Two purposes were intended for applying the reverse phase thin layer chromatography. First, to compare the chemical profile of ABC fraction on reverse phase and normal phase chromatography, and to find a proper mobile phase system able to isolate the target compounds on C18 silica gel.

After trying several mobile phase systems, separation of A, B and C compounds on reverse phase TLC plates was performed by using mobile phase contained methanol, acetonitrile (ACN) and water (35%, 35%, 30%, respectively). In addition to iodine vapour, the developed reverse phase plate was visualized by p-anisaldehyde and sulfuric acid.

Reverse Phase Column Chromatography

Amount of 0.5 g of each fraction obtained from normal phase column chromatography, i.e. Ab, aBc, and Cb, was subjected to column packed with 20 g of C18 silica gel (RP silica gel, Merck) and eluted with the same mobile phase indicated in a

previous step by reverse phase thin layer chromatography (35% MeOH, 35% ACN, 30% H_2O_2). A volume of 1.0 mL for was collected thru elution rate equal to 0.5 mL/min. After analyzing the collected fractions on reverse phase thin layer chromatography, a single band representing each of the compounds A (50.0 mg), B (78.0 mg), or C (25.0 mg) was shown indicating the successful isolation process. Subsequently, the isolated single compounds were injected into high performance liquid chromatography (HPLC) to confirm their purity.

High Performance Liquid Chromatography (HPLC)

Each of the isolated A, B and C compounds was submitted to reversed phase HPLC (Perkin-Elmer) on a Modern RP-HPLC Column (Zorbax Column Eclipse XDB C18, 5 µm, 4.6 x150 mm) and eluted with 35% MeOH, 35% ACN, and 30% H_2O_2. 1.0 mg of sample was dissolved in 1.0 mL of the mobile phase mixture and filtrated through 0.45µm filter syringe before it was automatically injected into the HPLC column. Injection volume was 10 µl, while the flow rate was 1ml/min, the detector was adjusted at wavelength 195 nm, and the analysis time was fixed to 10 min. The chromatograms demonstrated further injection of each compound was compared to that of ABC fraction.

Compounds Identification

Liebermann–Burchard Test

It was hypothesized that the butanol fraction composed mainly of saponin contents of *S. chloronotus* extract. Liebermann–Burchard reagent is a chemical indicator that reacts specifically with triterpene and steroids that form aglycone moieties of all saponins (Coelho & Alves, 1946). Accordingly, this test was used two times in the present study. The first time was to verify the presence of saponins in the active butanol fraction, while the second time was to demonstrate if the isolated active compounds are also saponin compounds. Liebermann-Burchard reagent was prepared by carefully mixing of 5 mL of acetic anhydride and 5 mL of concentrated sulfuric acid into 50 mL of absolute ethanol, while cooling in ice. A spot of each tested fraction or compound was applied on the TLC plate, and then it was sprayed with the prepared reagent and was heated at 100°C for 5–10 min. The positive reaction was indicated by appearance of blue colour under UV and visible light.

Spectroscopic Analysis

In order to identify structures of the isolated compounds A, B and C, they were analyzed by various spectroscopic analyses. ^{1}H, ^{13}C, and 2D NMR data were recorded at 400 MHz by BRUKER NMR, in Standards and Industrial Research Institute of Malaysia (SIRIM). The functional groups present in the isolated compounds were determined by infra-red (IR) spectra of the samples in KBr disc by using FT-IR. Molecular weights and fragmentation patterns were illustrated by mass spectra (MS) after molecular ionization by positive mode electron spray (+ES) method. ES-TOF-MS spectra were recorded by MS in University College London, UK.

Statistical Analysis

All experiments were carried out in triplicate, and the data were expressed as mean ± standard deviation. Significant differences between the groups were examined using t-test (Microsoft office excel, 2010). The differences were considered statistically significants when the p-values are less than 0.05

RESULTS

Cytotoxic Activities of Fractions and Subfractions of *S. chloronotus* Extract

Cytotoxic activities of all fractions obtained from liquid-liquid fractionation method were assessed by MTT viability test. The cytotoxic effect of each fraction at fixed concentration (20 µg/ml) was compared with the effect of the same concentration of the original methanol extract. As shown in Table 1, *n*-butanol fraction exhibited the highest cytotoxic effects, reducing the viability of A549 cells to 20.8%, and being more potent than the crude methanolic extract which reduced the viability of A549 cells to 43.5%. By applying 20µg/mL of dichloromethane fraction on A549 cells, their viability was reduced to 70% of the vehicle treated cells, demonstrating lower cytotoxic effect than the crude extract. On the other hand, none of the hexane, carbon tetrachloride, nor water fractions showed any significant effect on the viability of A549 cells.

Cytotoxic activities of the subfractions obtained from vacuum liquid chromatographic technique (VLC) of the active *n*-butanol fraction, i.e. BV10, BV20, BV30,… BV10, are displayed in Table 2. Only BV10 subfraction didn't show significant inhibition against A549 cells, while the subfractions B20 and B30 demonstrated mild to moderate cytotoxic effects, reducing the cell viability to 64.0% and 55.6% of the control cells, respectively. However, all the subfractions which were eluted by more than 40% methanol concentration, i.e. BV40, BV50, BV60,…, BV10, exhibited strong cytotoxic effects, reducing the cell viability to 27.0% and bellow.

Table 1: Cytotoxic activities of fractions and subfractions of *S. chloronotus* extract

Fractions	Weight (g)	% Cell Viability (at 20 µg/ml)	Cytotoxicity
Crude MeOH	41.0	43.5 ± 6.9	++
Hexane	2.0	95.9 ± 3.3	-ve
CCl_4	1.7	91.1 ± 8.7	-ve
DCM	4.3	69.9 ± 5.7	+
n-BuOH	16.5	20.8 ± 2.6	++++
H_2O	12.6	98.8 ± 4.0	-ve

Table 2: Cytotoxic activities of *n*-butanol subfractions of *S. chloronotus* extract

Fractions	% Cell Viability (at 20 µg/ml)	Cytotoxicity
BV10	88.8 ± 2.1	-
BV 20	64.0 ± 5.4	+
BV30	55.6 ± 4.7	++
BV40	27.0 ± 1.8	+++
BV50	24.6 ± 2.2	+++
BV60	18.4 ± 2.0	++++
BV70	7.1 ± 0.9	++++
BV80	10.5 ± 1.4	++++
BV90	11.4 ± 1.8	++++
BV100	16.6 ± 2.4	++++

Thin Layer Chromatography (TLC)

All the active subfractions were found to share three major bands on their chemical pattern on normal phase TLC plate. Therefore, they were collected together in one fraction (BVC), which was then subjected to size exclusion chromatography. Interestingly, the three bands (A, B and C) were isolated from the other fraction components and eluted together at the first collected fractions. After developing the mobile phase (8 $CHCl_3$: 2 MeOH: 0.1 H_2O) on normal phase TLC, the pattern of the active cytotoxic fraction (ABC) comparing to that of crude extract was illustrated in Figure 1. The values of retention factors (R_f) of the compounds A, B, and C were found to be 0.20, 0.17 and 0.10, respectively.

Furthermore, before complete isolation of the compounds A, B and C from each other by reverse phase column chromatography, a reverse phase TLC plate was developed to identify the proper mobile phase. Thus, the compounds A, B, and C were detected on reverse phase TLC by using a mobile phase composed of (35% MeOH, 35% ACN, and 30% H_2O_2), giving R_f values as followings (A: 0.25, B: 0.33, and C: 0.40). The distribution pattern of the isolated compounds A, B and C on the reverse phase TLC plate was demonstrated in (Figure 2, a and b).

High Performance Liquid Chromatography (HPLC)

HPLC was used to verify the purity of the isolated compounds. As shown in Figure 3, elution of ABC fraction through HPLC column by using a mobile phase (35% MeOH, 35% ACN, and 30% H_2O_2) demonstrated three major peaks representing the compounds A, B and C, at retention times 5.68 min., 4.62 min., and 4.08 min. respectively. Running same as the above mobile phase beyond injections of each isolated compound (A, B, and C) produced one corresponding major peak, in which compound C was eluted first at R_t = 4.08 min, followed by compound B at R_t = 4.65, and for compound A at R_t = 5.68 min.

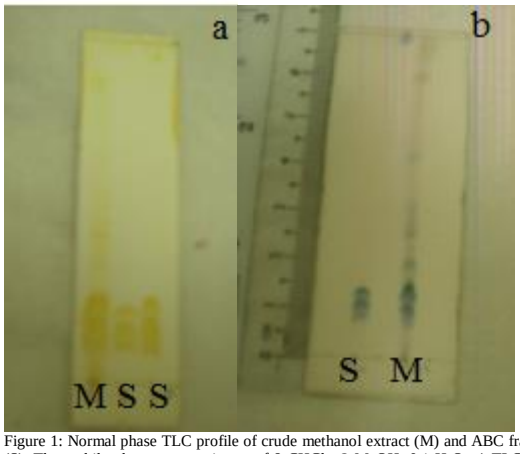

Figure 1: Normal phase TLC profile of crude methanol extract (M) and ABC fraction (S). The mobile phase was a mixture of 8 $CHCl_3$: 2 MeOH: 0.1 H_2O. a) TLC plate was visualized by exposure to iodine vapour; b) plate was visualized by spraying with p-anisaldehyde in glacial acetic acid.

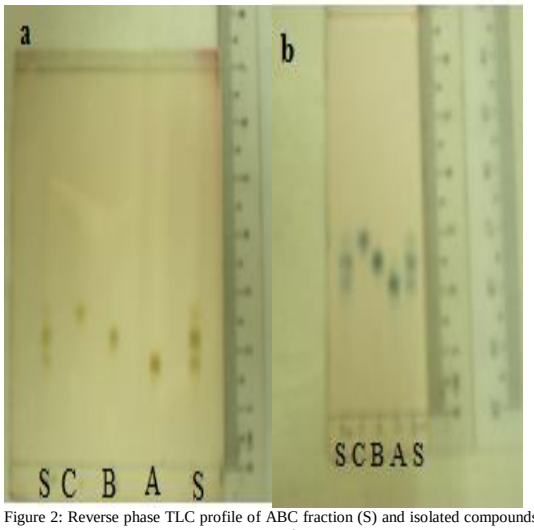

Figure 2: Reverse phase TLC profile of ABC fraction (S) and isolated compounds A, B, and C. The mobile phase was a mixture of 35% MeOH, 35% ACN, and 30% H_2O_2. a) TLC plate was visualized by exposure to iodine vapor; b) plate was visualized by spraying with p-anisaldehyde in glacial acetic acid.

Structural Identification of the Isolated Compounds

Liebermann–Burchard Test

Majority of the cytotoxic compounds previously isolated from sea cucumber species have been identified as triterpene glycosides (saponins). Thus, Liebermann–Burchard test was used to indicate if there were saponin components among the constituents of active butanol fraction. In addition, after completion of the isolation process, the three isolated compounds were tested by Liebermann–Burchard reagents to verify if they are saponins, specifically containing triterpenes in their structures. A crude butanol fraction in addition to each individual compound (A, B, and C) demonstrated positive reaction with Liebermann–Burchard reagent suggesting that the active cytotoxic compounds in *S. chloronotus* are saponins. As shown in (Figure 4), the positive reactions were verified by formation of a dark blue colour upon heating the reagent with tested compounds.

Spectroscopic Analysis

Infra Red Spectra (IR)

As shown in the Figures S1, S13, and S27, the three isolated compounds showed almost the same typical absorption bands in their IR spectrum, indicating that they possess the same functional groups. Each of the compounds A, B and C demonstrated strong hydroxyl absorption at 3400 cm^{-1} (broad) as well as a carbonyl absorption band at 1735 cm^{-1} (broad) indicating the presence of the characteristic γ-lactone and an acetyl group. Furthermore, presence of sulphate (S-O) group was indicated by appearance of absorption bands at (1245, and 1071) cm^{-1}.

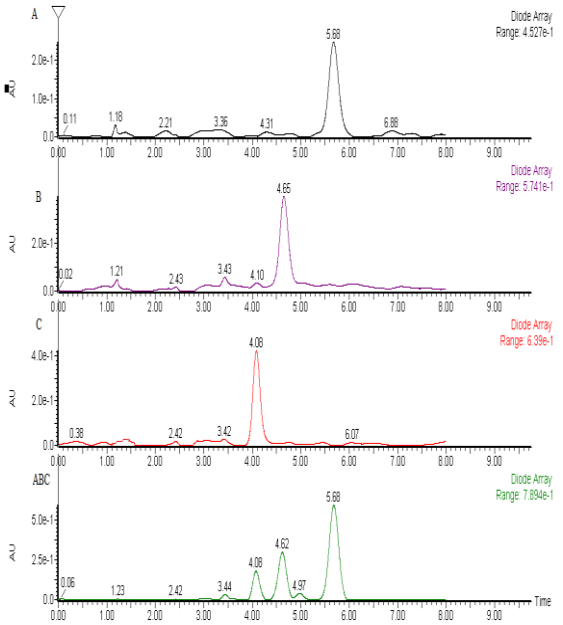

Figure 3: HPLC profile of the isolated compounds A, B and C, and the fraction ABC. The mobile phase was a mixture of 35% MeOH, 35% ACN, and 30% H_2O_2.

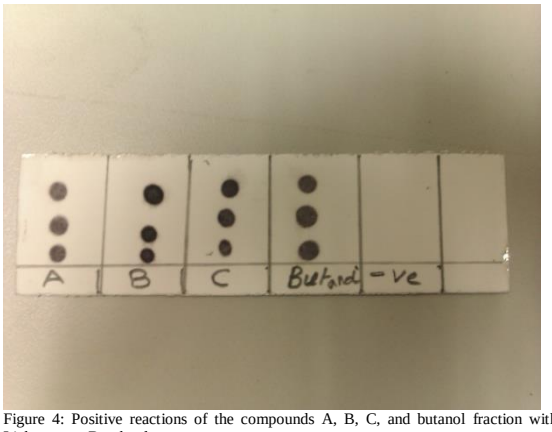

Figure 4: Positive reactions of the compounds A, B, C, and butanol fraction with Liebermann–Burchard reagent.

Nuclear Magnetic Resonance Spectra (NMR)

The ^{13}C-NMR and DEPT spectra of the compounds A, B and C revealed the presence of 66, carbon atoms in each compound. The DEPT spectra of compound A demonstrated the presence of 11 methyls (CH_3), 14 methylenes (CH_2), 34 methines (CH), and 7 quaternary carbons (C) (Figures S6 and S7). Compound B was found to contain 10 methyls, 15 methylenes, 34 methine, and 7 quaternary carbons (Figures S19-S21). On the other hand, the 66 carbons of compound C consisted of 9 CH_3, 16 CH_2, 33 CH, and 8 quaternary (C) (Figures S34 and S35). Furthermore, ^{13}C-NMR of the three compounds were found to be highly similar to that demonstrated by stichoposide E (or called stichloroside A_1), an antifungal triterpene glycoside isolated earlier from *S. chloronotus* species collected from the Australian littoral (Mal'tsev et al., 1983).

As shown in Table 3, an identical ^{13}C-NMR chemical shift and DEPT data of aglycone moiety of stichoposide E were found in that of the compounds A and B. Their ^{13}C and ^{1}H NMR spectra revealed the presence of holostane nucleus which is common in most tritepene glycosides isolated from sea cucumbers. ^{13}C-NMR of both A and B compounds possessed resonances due to one olefinic double bond at the tertiary and quaternary carbons (C7, δ_C 119.4 ppm and C8, δ_C 146.8 ppm) and one lactone carbonyl group (C18, δ_C 180.0 ppm). In addition, the ^{13}C-NMR spectra demonstrated the signals

characteristic for the presence of C23 (δ_C 68.2 ppm) acetoxy group ($OCOCH_3$) at δ_C 170.6 ppm for the quaternary carbon, and at 21.6 ppm for the methyl carbon. In the aliphatic side chain, the signals of two methyl groups (C26, C27) attached to a methine carbon (C25, δ_C 24.3ppm) appeared at 22.3 and 23.5 ppm, respectively. Similar to stichoposide E, additional 5 methyl groups attached to the holostane skeleton were indicated by the signals at chemical shifts δ_C 24.0 (C19), δ_C 26.9 ppm (C21), δ_C 16.9 ppm (C30), δ_C 28.4 ppm (C31), and δ_C 30.4 ppm (C32) in ^{13}C-NMR spectra of the glycosides A and B. However, a signal of C3 was masked by the solvent (DMSO-d6) signals at δ_C 39.0-40.0 ppm.

Table 3: ^{13}C NMR data of the aglycone moieties of the compounds A, B, C and stichoposide E

	***Stichoposide E		Compound A		Compound B		Compound C	
Position	**δ ppm**	**DEPT**	***δ ppm**	**DEPT**	***δ ppm**	**DEPT**	***δ ppm**	**DEPT**
1	35.9	CH_2	36.0	CH_2	36.1	CH_2	36.1	CH_2
2	27.0	CH_2	26.9	CH_2	26.7	CH_2	26.8	CH_2
3	88.8	CH	88.9	CH	88.5	CH	88.7	CH
4	39.9	C	**	**	**	**	**	**
5	47.8	CH	47.6	CH	47.6	CH	47.1	CH
6	22.5	CH_2	22.7	CH_2	22.4	CH_2	22.7	CH_2
7	119.4	CH	119.4	CH	119.5	CH	119.5	CH
8	146.4	C	146.5	C	146.6	C	146.5	C
9	47.1	CH	47.0	CH	47.1	CH	47.5	CH
10	35.2	C	35.2	C	35.3	C	35.3	C
11	22.8	CH_2	22.9	CH_2	22.7	CH_2	22.9	CH_2
12	30.4	CH_2	30.0	CH_2	30.0	CH_2	29.9	CH_2
13	58.2	C	58.1	C	58.2	C	58.2	C
14	51.0	C	51.1	C	51.1	C	51.0	C
15	33.9	CH_2	34.0	CH_2	34.0	CH_2	34.1	CH_2
16	24.6	CH_2	24.5	CH_2	24.5	CH_2	24.5	CH_2
17	54.3	CH	53.7	CH	53.7	CH	53.6	CH
18	180.0	C	179.8	C	179.8	C	179.8	C
19	23.9	CH_3	24.0	CH_3	24.0	CH_3	24.0	CH_3
20	83.3	C	83.4	C	83.5	C	83.4	C
21	26.7	CH_3	26.9	CH_3	26.9	CH_3	26.9	CH_3
22	44.0	CH_2	43.5	CH_2	43.6	CH_2	42.8	CH_2
23	68.1	CH	68.2	CH	68.2	CH	68.5	CH
24	44.9	CH_2	44.9	CH_2	44.9	CH_2	44.3	CH_2
25	24.3	CH	24.3	CH	24.3	CH	**141.7**	**C**
26	22.3	CH_3	22.3	CH_3	22.3	CH_3	22.5	CH_3
27	23.2	CH_3	23.4	CH_3	23.5	CH_3	**114.4**	**CH_2**
28	170.8	C	170.6	C	170.6	C	170.3	C
29	21.4	CH_3	21.6	CH_3	21.6	CH_3	21.5	CH_3
30	16.9	CH_3	17.2	CH_3	17.3	CH_3	17.3	CH_3
31	28.4	CH_3	28.6	CH_3	28.7	CH_3	28.7	CH_3
32	30.9	CH_3	31.2	CH_3	31.3	CH_3	31.2	CH_3

*Recorded at 400 MHz in DMSO-d6, **the signal was overlapped with solvent signals. *** As reported by Mal'tsev et al. (1983).

2 D NMR (HMQC, HMBC, and ^{1}H -^{1}H COSY) experiments were employed to assign the protons to their corresponding carbons and to correlate most of the proton signals in both aglycone and carbohydrate moieties. HMQC was used to establish one-bond carbon–proton connectivity (Figures S9, S22, and S36), by which all the proton resonances were correlated with those of their corresponding carbons (Tables 4-9). Proton–proton connectivities were established using COSY experiment (Figures S12, S26, and S39), while HMBC was used to establish long-range (2- or 3-bond) carbon– proton connectivities (Figures S10, S11, S23, S24, S37 and 38). COSY spectra of the isolated compounds allowed to determine the position of the double bond at C7 (δ_C 119.4 ppm), which was indicated by the correlation between a signal of C7 proton (δ_H 5.50) with those of C6 protons (δ_H 1.87 ppm) in COSY spectra. In addition, binding of acetoxy group to C23 (δ_C 68.2 ppm) was confirmed by the cross peaks between proton at C23 position (δ_H 5.12 ppm) and those of C22 (δ_H 2.02 ppm) and C24 position (δ_H 1.50 ppm) in COSY spectra. Furthermore, attachment positions of the five methyl groups to the holostane skeleton were confirmed from the long correlations between methyl protons and the carbon atoms in the holostane nucleus by HMBC experiment. Protons at C19 (δ_C 24.0, δ_H 0.91s) exhibited strong correlation with C10 (δ_C35.2 ppm), while the protons at C21 (δ_C 26.9 ppm, δ_H 1.36 s ppm) were correlated with C20 (δ_C 83.4 ppm), protons at C30 (δ_C 17.2 ppm, δ_H 0.85 ppm) and methyl proton at C31 (δ_C 28.6 ppm, δ_H 1.12 ppm) to C4 (δ_C 39.7 ppm), and finally protons at C32 (δ_C 31.2 ppm, δ_H 1.15 ppm) to C14 (δ_C 51.1 ppm) in HMBC spectra. Based on the above data, the similar structure of the aglycone parts of the compounds A and B was identified as 23-acetoxy-holosta-7-en-3β-ol.

Table 4: ^{13}C and ^{1}H NMR chemical shifts and selected HMBC correlations for the aglycone moiety of compound A

Position	***δ_C ppm**	**DEPT**	***δ_H ppm mult. (*J* in Hz)**	**HMBC**
1	36.0	CH_2	1.35 m	-
2	26.9	CH_2	1.50 m	-
3	88.9	CH	3.04 m	-
4	**	**		-
5	47.6	CH	0.87 m	-
6	22.7	CH_2	1.87 m	-
7	119.4	CH	5.55 brd	-
8	146.5	C		-
9	47.0	CH	3.14 m	-
10	35.2	C		-
11	22.9	CH_2	1.75 brd	-
12	30.0	CH_2	2.02 brd	-
13	58.1	C		-
14	51.1	C		-
15	34.0	CH_2	1.40 m	-
16	24.5	CH_2	1.02 m	-
17	53.7	CH	2.33 d (5.2)	-
18	179.8	C		-
19	24.0	CH_3	0.91 s	C: 1,5,9,10
20	83.4	C		-
21	26.9	CH_3	1.36 s	C: 17,20,22
22	43.5	CH_2	2.02 m	-
23	68.2	CH	5.12 brd	-
24	44.9	CH_2	1.48 m	C26
25	24.3	CH	1.05 m	-
26	22.3	CH_3	0.87 s	C: 24,25,27
27	23.4	CH_3	0.86 s	C: 26,C24
28	170.6	C		-
29	21.6	CH_3	1.99 s	C28
30	17.2	CH_3	0.88 s	C: 3,4,5,31
31	28.6	CH_3	1.01 s	C: 3,4,5,30
32	31.2	CH_3	1.07 s	8,13,14,15

*Recorded at 400 MHz in DMSO-d6, **The signal overlapped with solvent signals. (singlet); d (doublet); dd (doublet of doublet), t (triplet); m (multiplet), brd (broad)

Table 5: ^{13}C and ^{1}H NMR chemical shifts and HMBC correlations for the sugar moieties of compound A

Sugar Units	**Carbon No.**	***δ_C ppm**	**DEPT**	***δ_H ppm mult. (*J* in Hz)**	**HMBC**
Xylose I	1	104.3	CH	4.32 d (6.0)	aglycone C3
	2	82.4	CH	3.35 m	C1 Qu
	3	74	CH	3.15 m	C1
	4	76.9	CH	3.20 m	-
	5	61.2	CH_2	3.71 m	-
Quinovose	1	104.1	CH	4.48 d (7.6)	C2 xyl I
	2	76.3	CH	3.24 m	-
	3	75	CH	3.53 m	-
	4	85	CH	3.05 m	C5
	5	70.8	CH	3.5 m	-
	6	17.7	CH3	1.23 d (4.8)	C5,C4
					-
Xylose II	1	104.35	CH	4.37 d (7.6)	C4 Xyl I
	2	72.1	CH	3.32 m	C1, C2
	3	87.7	CH	3.35 m	C2,3,
	4	68.4	CH	3.45 m	-
	5	61.5	CH_2	3.66 m	-
Xylose III	1	104.5	CH	4.40 d (6.8)	C4 Quin.
	2	72.3	CH	3.34 m	C2,3,
	3	87.7	CH	3.43 m	C1, C2
	4	68.8	CH	3.46 m	-
	5	61.4	CH_2	3.69 m	-
Met-xyl	1	101.2	CH	4.35	C2,C3 Xyl II
	2	74.3	CH	3.14 m	C1,C3
	3	86.4		2.99 m	C2,C4, OCH_3
	4	69.7	CH	3.18 m	C1, C3
	5	63.4	CH_2	3.69 m	-
	OCH_3	CH3	OCH_3	3.48 s	C3
Met-Glc	1	103.6	CH	4.51 d (7.6)	C2, C3 Xyl III
	2	75.5	CH	3.21 m	C1, C3
	3	86.4	CH	2.98 m	C2,C4, OCH_3
	4	69.8	CH	3.19 m	-
	5	77.2	CH	3.15 m	-
	6	65.1	CH_2	3.85 m	-
	OCH_3	CH3	CH_3	3.48 s	C3

*Recorded at 400 MHz in DMSO-d6. s (singlet); d (doublet); dd (doublet of doublet), t (triplet); m (multiplet), brd (broad)

On the other hand, the ^{13}C-NMR spectrum of aglycone moiety of compound C was found to be slightly different from those of compounds A, B and stichoposide E. The exceptional signals in

the compounds C were ascribed to presence of a 25(27)-double bond in the side chain (Δ^{25}). This was concluded from the downfield shifting of C25 and C27 from δ_C 24.3 ppm and δ_C 23.5 ppm, to δ_C 141.7 ppm and δ_C 114.4 ppm, respectively. In addition, DEPT signals of C25 and C27 changed from being CH (C25) and CH_3 (C27), to be quaternary (C) and methylene (CH_2) carbons, respectively (Table 8). Likewise, the correlated protons of the carbons (C24, 26, and 27) were shifted downfield from being at (δ_C 1.48 ppm, 0.85 ppm, and 0.85 ppm, respectively) in the compound A and B to be found at (δ_C 2.41 ppm, 1.72 ppm, and 4.80 ppm, respectively). Therefore, the structure of the aglycone moiety of the compound C was identified as 23-acetoxy-holosta-7,25-dien-3β-ol. Similar to this aglycone structure was found to be attached to hexasaccharide chain in stichloroside A_2, another antifungal triterpene glycoside isolated early from *S. chloronotus* (Kitagawa, Nishino, et al., 1981).

The sugar moieties of the isolated glycosides A, B and C, consisted of six monosaccharide residues as deduced from the ^{13}C-NMR spectrum (Figures S7, S19 and 34), which showed the signals of six anomeric carbons in each glycoside at 101-105 ppm (Table 5). HMQC spectrum verified that the anomeric carbons were correlated with the corresponding signals of anomeric protons at δ_H 4.3-4.5 ppm. The relative large coupling constants of the anomeric protons ($J \approx 7.6$ Hz) were indication for *β*-configuration of the glycosidic bonds in all cases (Figure S9). Unlike the aglycone moieties, the three isolated compounds exhibited different ^{13}C and ^{1}H-NMR spectra of the sugar moities from those found in stichloroside A_1 and A_2. However, the sugar moieties of the compounds B and C exhibited identical ^{13}C and ^{1}H-NMR spectra, indicating that they both bear the same carbohydrate units which are partially different from those in compound A.

The presence of six monosaccharide units in the sugar chain of the glycoside A was deduced from its ^{13}C-NMR, ^{1}H-NMR and DEPT spectra (Table 5). These spectra showed six signals in the characteristic region of anomeric carbons (101.2 ppm, 103.6 ppm, 104.1 ppm, 104.3 ppm, 104.4 ppm and 104.5 ppm) correlated to six doublet anomeric protons at 4.3-4.5 ppm in the HMQC spectrum (Figure S9). In addition to the six anomeric carbons, sugar moiety of the compound A was found to contain 20 methines CH (δ_C = 68.4-87.7 ppm), five methylenes (δ_C = 61.2-65.1 ppm), one methyl (δ_C = 17.7 ppm), and two overlapped methyl of methoxy groups (δ_C = 60.4 ppm). The presence of total of 35 carbons with this DEPT signals distributed in six sugar units suggested that hexasaccharide chain of the glycosides A is composed of four ribose and two hexose sugars, in which two sugar units bear methoxy groups. The signal of methyl carbon at δ_C (17.7 ppm) and its corresponding doublet protons at (δ_H 1.3, J= 4.8) suggested the presence of deoxygenated sugar (quinovose). This was supported by the presence of only five oxygenated CH_2 at δ_C = 61.2-65.1 ppm, in the six sugar units of the proposed hexasaccharide chain (Table 5). Considering the fact that the carbohydrate chains of sea cucumber triterpene glycosides contain only xylose, quinovose, glucose, 3-*O*-methylglucose, and 3-*O*-methylxylose (Caulier et al., 2011), it was postulated that the hexasaccharide chain of the glycoside A is composed of three xyloses, one quinovose, one 3-*O*-methylglucose, and lastly one 3-*O*-methylxylose. This was also supported by comparison of ^{13}C NMR data of the carbohydrate moieties in compound A with those of sea cucumber triterpene glycosides that contain xyloses, quinovose, 3-*O*-methylglucose, and 3-*O*-methylxylose (Silchenko et al., 2002).

Moreover, the positions of the interglycosidic linkages were deduced from HMBC spectra, where cross-peaks between H-1 of the first monosaccharide residue (xylose I) and C-3 of an aglycone, H-1 of the second monosaccharide residue (quinovose) and C-2 of the xylose I, H-1 of the xylose II and C-4 of the xylose I, H-1 of the 3-*O*-methylxylose and C-3 of the xylose II, and H-1 of the fifth monosaccharide residue (xylose III) C-4 of the quinovose, H-1 of the *3-O*-methylglucose and C-3 of the xylose III were observed (Figure 5). D-configuration of the six carbohydrate units was assumed according to that most often encountered among the sea cucumber glycosides (Caulier et al., 2011). In addition, the proposed carbohydrate sequence in the compound A was supported by its fragmentation pattern in the electrospray mass spectra (ESI-TOF-MS) (Figures 6 & 7).

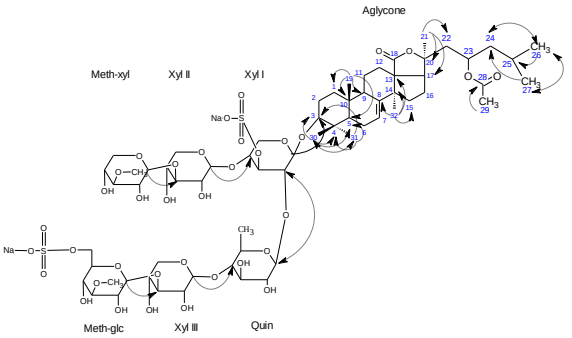

Figure 5: Selected key HMBC correlations of compound A

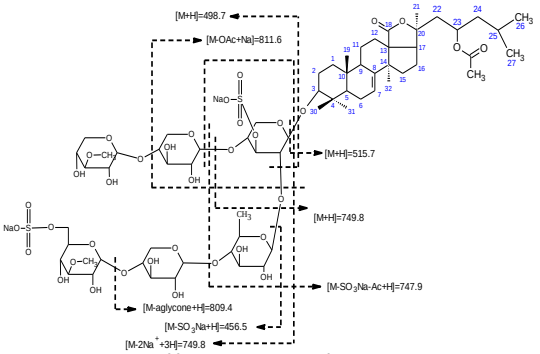

Figure 6: Interpretation of fragmentation pattern of compound A in +ESI-TOF-MS.

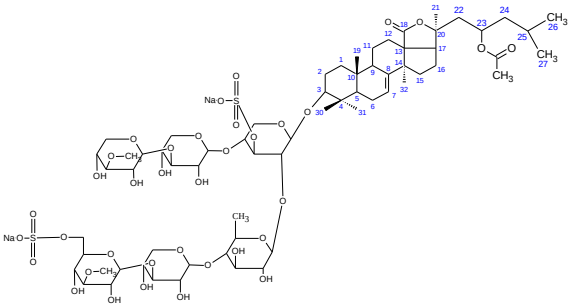

Figure 7: Proposed structure of compound A.

The high resolution electrospray mass spectra (HR ESI-TOF-MS) (positive ion mode) of the glycoside A exhibited a pseudo molecular ion peak [M - Ac + H^+] at *m/z* 1541.56. The molecular formula of the pseudo molecular ion was calculated as $C_{64}H_{102}O_{35}SNa_2$, that allowed the determination of molecular formula for the glycoside A as C_{66} $H_{104}Na_2O_{36}S_2$ (calculated molecular weight = 1583.62 Da). In the + ESI- MS of the glycoside A, the ion peaks [M + Na] at *m/z* 1461.64 indicated the loss of a sulphate group along with acetyl group. In addition, the major peak [M + H] observed at *m/z* 337.26 was referred to a fragment of the first two xyloses with sodium sulphate group (Figure 6).

As was mentioned above, the consequence of the carbohydrate units in glycoside A was confirmed also with the aid of the fragmentation pattern in the +ESI-TOF-MS spectrum. As shown in Figure 6, the presence of two successive xylose units attached to the triterpenoid aglycone moiety was indicated by the two major peaks observed at [M - OAc + Na] *m/z* 811.62, while attachment of the first xylose to quinovose residue and the aglycone moiety was deduced from the peak [M – SO_3Na - Ac + H] at *m/z* 747.9. In addition, the common attachment of xylose sugar to sodium sulphate group and the triterpenoid aglycone was confirmed by [M + H] peak at *m/z* 749.8. Loss of terminal 3-*O*-methylglucose along with its attached sodium sulphate group was indicated by the peak [M + H] at *m/z* 809.47.

Furthermore, the presence of xylose-quinovose-3-*O*-methylglucose sequence in the carbohydrate chain was indicated by the peak [M + H] at *m*/*z* 456.56, while the sequence of the sodium sulphated xylose-xylose-3-*O*-methylxylose was determined at [M + H] *m*/*z* 498.4. All this data suggested the structure of the glycoside A as holostane triterpenoid attached to hexasaccharide sugar as illustrated in Figure. 7.

The sugar part of compound B was found to contain a total of 34 carbons, including six anomeric carbons at δ_C =101.2-104.8 ppm, 20 other methines (δ_C 68.2- 87.8 ppm), six methylenes (δ_C 61.2-65.7 ppm), and two methoxy group (δ_C 60.4 ppm) (Table 6). This suggested the presence of six sugar units including 2 hexoses (mainly glucose), and 4 pentoses (mainly xylose), while two of the sugar residues were attached to methoxy groups (Table 7 and Figure S19). Unlike glycoside A, there were no signals indicating the presence of quinovose sugar among the carbohydrate chain of glycoside B. This also was supported by comparison of the ^{13}C NMR spectra of compound B with those of published glycosides containing xylose and 3-*O*-methylglucose in their carbohydrate moieties (Kalinin et al., 2008; Silchenko et al., 2002)

Table 6: ^{13}C and ^{1}H NMR chemical shifts and selected HMBC correlations for the aglycone moiety of compound B

Position	*δ_C ppm	DEPT	*δ_H mult. (*J* in Hz)	HMBC
1	36.1	CH_2	1.34 m	-
2	26.7	CH_2	1.50 m	-
3	88.5	CH	3.04 t brd (8)	-
4	**	**		-
5	47.6	CH	0.87 m	-
6	22.4	CH_2	1.88 m	-
7	119.5	CH	5.49 dd (3.6,2.8, 12)	-
8	146.6	C		-
9	47.1	CH	3.14 m	-
10	35.3	C		-
11	22.7	CH_2	1.75 m	-
12	30.0	CH_2	2.03 m	-
13	58.2	C		-
14	51.1	C		-
15	34.0	CH_2	1.39 m	-
16	24.5	CH_2	1.03 m	-
17	53.7	CH	2.33 d brd (5.6)	-
18	179.8	C		-
19	24.0	CH_3	0.91 s	C: 1,5,9,10
20	83.5	C		-
21	26.9	CH_3	1.36 s	C:17,20,22
22	43.6	CH_2	2.02 d brd (14)	-
23	68.2	CH	5.14 m	-
24	44.9	CH_2	1.49 m	C26
25	24.3	CH	1.0	-
26	22.3	CH_3	0.85 s	C: 24,25,27
27	23.5	CH_3	0.86 s	C: 26,C24
28	170.6	C		-
29	21.6	CH_3	2.0 s	C28
30	17.3	CH_3	0.88 s	C: 3,4,5,31
31	28.7	CH_3	1.02 s	C: 3,4,5,30
32	31.3	CH_3	1.07 s	C:8,13,14,15,16

*Recorded at 400 MHz in DMSO-d6, **The signal was overlapped solvent signals. (singlet); d (doublet); dd (doublet of doublet), t (triplet); m (multiplet), brd (broad)

The interglycosidic linkages in the hexasaccharide chain compound B and its bonding to the aglycone were established by HMBC experiments (Figure 8), which showed cross-peaks between H-1 of the first xylose and C-3 of the aglycone, H-1 of second xylose and C-2 of the first xylose, H-1 of xylose III and C-4 of xylose I, H-1 of 3-*O*-methylglucose I and C-3 of the xylose III, H-1 of xylose IV and C-4 of xylose II residue, and H-1 of 3-*O*-methylglucose II and C-3 of the xylose III. Furthermore, the proposed monosaccharide contents and their sequence were also confirmed by the fragmentation pattern +ESI-TOF-MS data (Figures 9 & 10).

The glycoside B exhibited a pseudo molecular ion peak [M - OSO_3Na - Na + 2H] at *m*/*z* 1561.24 in the HR ESI-TOF-MS (positive ion mode), suggesting the molecular formula as $C_{66}H_{105}NaO_{36}S_2$. The calculated molecular weight of glycoside B was 1701.66 with molecular formula as $C_{66}H_{103}Na_3O_{40}S_3$. This was supported by the presence of the pseudo molecular peaks [M -OSO_3Na - 2Na + 3H] and [M - SO_3Na - 2Na + 3H] at *m*/*z* 1539.6 and 1555.6 respectively. The major peak [M – 2Na + 3H] at *m*/*z* 1482.2 suggested detachment of one OSO_3Na and acetyl groups (Figure 9).

Table 7: ^{13}C and ^{1}H NMR chemical shifts and HMBC correlations for the sugar moiety of compound B

Sugar Unit	Carbon No.	*δ_C ppm	DEPT	*δ_H mult. (*J* in Hz)	HMBC
Xylose I					
	1	104.2	CH	4.3625 (8.4)	C3
	2	81.9	CH	3.45m	-
	3	74.1	CH	3.29 m	C1,2,4
	4	76.5	CH	3.62 m	-
	5	61.2	CH_2	3.69 m	-
Xylose II					
	1	101.2	CH	4.33 d (7.2)	C2 Xyl I
	2	74.4	CH	3.29 m	C1
	3	74.8	CH	3.21m	C2,4,5
	4	76.9	CH	3.62 m	C2,3,4
	5	61.3	CH_2	3.69 m	-
Xylose III					
	1	104.2	CH	4.3745 (7.6)	C4 Xyl I
	2	72.1	CH	3.29 m	C1
	3	68.4	CH	3.32 m	C2,3,
	4	87.4	CH	3.43 m	-
	5	61.5	CH_2	3.69 m	-
Xylose IV					
	1	104.7	CH	4.39 (6.4)	C4 Xylose2
	2	72.4	CH	3.29 m	C1
	3	68.8	CH	3.34 m	C2,3,
	4	87.7	CH	3.43 m	-
	5	61.4	CH_2	3.69 m	-
Meth-Glc I					
	1	101.2	CH	4.41 (7.2)	C3 Xyl III
	2	75.6	CH	3.22 m	C2,3,OCH_3
	3	86.5	CH	2.98 t brd (8.8)	C2,C4,C5, OCH_3,
	4	69.8	CH	3.19 m	C2,3, OCH_3
	5	77.2	CH	3.21 m	-
	6	63.3	CH_2	3.69 m	-
	OCH_3	60.4	CH_3	3.48 s	-
Meth-Glc II					
	1	103.4	CH	4.51 (7.6)	C3 Xyl IV
	2	75.7	CH	3.22 m	-
	3	86.5	CH	2.98 t brd (8.8)	C1,2,C4,C5, OCH_3
	4	70	CH	3.19 m	-
	5	79.7	CH	3.41 m brd	-
	6	65.6	CH_2	3.85 m	-
	OCH_3	60.4	CH_3	3.48 s	C3

*Recorded at 400 MHz in DMSO-d6. (singlet); d (doublet); dd (doublet of doublet), t (triplet); m (multiplet), brd (broad)

Similar to glycoside A, the fragmentation pattern of glycoside B was employed to confirm the contents and the sequence of the carbohydrate residues (Figure 9). The peaks observed at *m*/*z* 515.37 and 455.35 were attributed to the aglycone triterpenoid fragments [M + H] and [M - OAc +H], respectively. The presence of two 3-*O*-methylglucoses at both terminal sites of the chain was confirmed by the two peaks appearing at *m*/*z* 809.6 and 649.4, which were attributed to the deattachment of one and two 3-*O*-methylglucose residues and their attached sulphate from the carbohydrate chain. Furthermore, similar to that shown in the + ESI-TOF-MS of glycoside A, the peak at *m*/*z* 747.3 confirmed attachment of the xylose residue to sulphate group and the triterpenoid aglycone. Based on the NMR and ESI-TOF-MS spectra, the structure of glycoside B was postulated as illustrated in Figure 10.

The signals in ^{13}C-NMR spectra ascribed to the carbohydrate residues of compound C were identical to those of compound B, indicating the presence of same carbohydrate units in both glycosides. Similar to compound B, the 34 carbons in the sugar parts of compounds C were identified as six methine anomeric carbons (δ_c = 101-105 ppm), 20 methines (δ_c = 67.8-88.7 ppm), six methylenes (δ_c = 61.2-65.1 ppm) and two methoxy groups (δ_c = 60.4 ppm) (Table 8 and Figure S34). This data suggested the presence of six carbohydrate units including four xyloses and two terminal 3-*O*-methylglucoses (Table 9).

A careful analysis of the HMBC spectra of the carbohydrate moieties in compound C, starting from the characteristic anomeric proton signals, allowed identifying the sugar sequence and the location of the interglycosidic linkage (Figure 11). The cross peaks exhibited in the HMBC spectra between H-1 of the

first xylose and C-3 of the aglycone confirmed the common position of the glycosidic linage between the aglycone and carbohydrate moieties of compound C. On the other hand, the cross peeks between H1 of second xylose and C2 of the first xylose, H1 of xylose III and C4 of xylose I, H1 of 3-*O*-methylglucose I and C3 of the xylose III, H1 of xylose IV and C4 of xylose II residue, and H-1 of 3-*O*-methylglucose II and C3 of the xylose III confirmed the sequence of the sugar units. This also was confirmed by interpretation of the +ESI-TOF-MS spectra of the compound C (Figures 12 and 13).

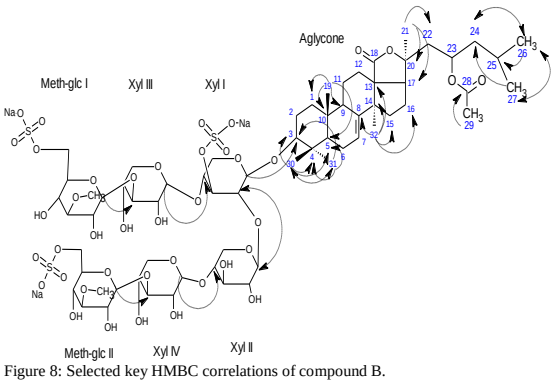

Figure 8: Selected key HMBC correlations of compound B.

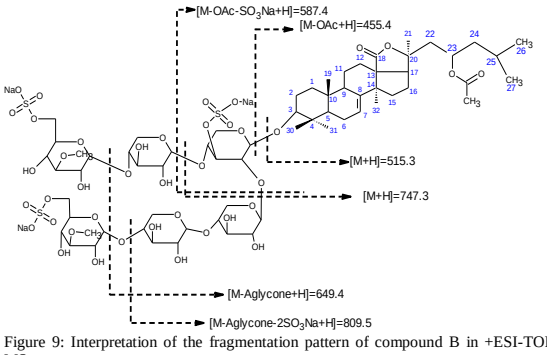

Figure 9: Interpretation of the fragmentation pattern of compound B in +ESI-TOF-MS.

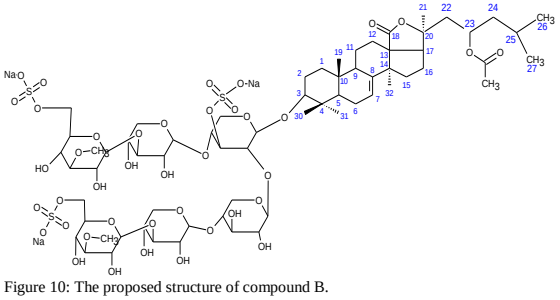

Figure 10: The proposed structure of compound B.

The glycoside C exhibited pseudo molecular ion [M - Ac - 4Na + 5H] at *m/z* 1671.38 that was used to calculate the molecular weight of the glycoside C as M= 1801.69 Da, suggesting the chemical formula as $C_{66}H_{100}Na_4O_{43}S_4$ (Figure 12). This suggested that the only difference between the carbohydrate moieties of the compound C and B is the presence of extra sulphate group in C3 of xylose II in compound C. Existence of two successive sulphated xyloses attached to the aglycone moiety was confirmed by the peak [M + H] demonstrated at 981.30 *m/z*, while attachement of two sulphated xyloses to third one (assumed as Xyl I, II and III) and the aglycone was suggested by the major peak [M + H] at *m/z* 1097.35. The major peak [M - OAc + Na] at *m/z* 1207.94 suggested detachment of the two 3-*O*-methylglucoses with their attached sulphate groups, indicating that they were two terminal residues of the carbohydrate chain. Furthermore, the presence of carbohydrate chain in a sequence of sulphated 3-*O*-methylglucose -xylose III- sulphated xylose I attached to the aglycone part was deduced from the peak [M- OAc - Na + 2H] appeared at *m/z* 1059.51 (Figure 12). Therefore, the structure of the compound C was proposed as shown in Figure 13.

Table 8: ^{13}C and ^{1}H NMR chemical shifts and selected HMBC correlations for the aglycone moiety of compound C

Position	***δ_C ppm**	**DEPT**	***δ_H mult. (*J* in Hz)**	**HMBC**
1	36.1	CH_2	1.34 m	C: 19,2
2	26.8	CH_2	1.47 m	C: 1,3,
3	88.7	CH	3.05 dd (6.8,14)	C: xylose2, xylose1
4	**	**		
5	47.1	CH	0.92 m	-
6	22.7	CH_2	1.89 d brd (13.5)	-
7	119.5	CH	5.55 s brd	-
8	146.5	C		-
9	47.5	CH	3.13 t brd (7.6)	-
10	35.3	C		-
11	22.9	CH_2	1.75 s brd	-
12	29.9	CH_2	2.03 s brd	-
13	58.2	C		-
14	51.0	C		-
15	34.1	CH_2	1.07 m	-
16	24.5	CH_2	1.03 m	-
17	53.6	CH	2.35 dd (4.1,8.5)	-
18	179.8	C		-
19	24.0	CH_3	0.91 s	C:1,5,9,10
20	83.4	C		-
21	26.9	CH_3	1.37 s	C:17,20,22
22	42.8	CH_2	1.9 m	-
23	68.5	CH	5.17 m	C:20
24	44.3	CH_2	2.24 d brd (7.2)	C:23,25,26,27
25	**141.7**	C		-
26	22.5	CH_3	1.71 s	C:24,25,27
27	**114.4**	CH_2	4.73, 4.79 s brd	C:26,C24
28	170.3	C		-
29	21.5	CH_3	1.97 s	C:23,28
30	17.3	CH_3	0.85 s	C:3,4,5,31
31	28.7	CH_3	0.91 s	C: 3,4,5,30
32	31.2	CH_3	1.02 s	C: 8,13,14,15,16

*Recorded at 400 MHz in DMSO-d6, **The signal was overlapped with solvent signals. (singlet); d (doublet); dd (doublet of doublet), t (triplet); m (multiplet), brd (broad)

Table 9: ^{13}C and ^{1}H NMR chemical shifts and HMBC correlations for the sugar moiety of compound C

Sugar Units	**Carbon No.**	***δ_C ppm**	**DEPT**	***δ_H mult (*J* in Hz)**	**HMBC**
Xylose I					
	1	104.3	CH	4.3625 (8.4)	C3
	2	81.7	CH	3.45m	-
	3	74.5	CH	3.29 m	C1,2,4
	4	76.7	CH	3.62 m	-
	5	61.2	CH_2	3.69 m	-
Xylose II					
	1	104.1	CH	4.33 d (7.2)	C2 Xyl I
	2	74.5	CH	3.29 m	C1
	3	74.8	CH	3.21m	C2,4,5
	4	76.9	CH	3.62 m	C2,3,4
	5	61.4	CH_2	3.69 m	-
Xylose III					
	1	104.3	CH	4.3745 (7.6)	C4 Xyl I
	2	72.2	CH	3.30 m	C1
	3	87.5	CH	3.32 m	C2,3,
	4	67.8	CH	3.43 m	-
	5	61.5	CH_2	3.69 m	-
Xylose IV					
	1	104.5	CH	4.39 (6.4)	C4 Xyl II
	2	72.4	CH	3.30 m	C1
	3	87.8	CH	3.34 m	C2,3,
	4	68.9	CH	3.43 m	-
	5	61.6	CH_2	3.69 m	-
Met-Glc I					
	1	101.3	CH	4.41 (7.2)	C3 Xyl III
	2	75.5	CH	3.22 m	C2,3, OCH_3
	3	86.5	CH	2.98 t brd (8.8)	C2,C4,C5, OCH_3
	4	69.7	CH	3.19 m	C2,3,OCH_3
	5	77.2	CH	3.21 m	-
	6	63.3	CH_2	3.69 m	-
	OCH_3	60.4	CH_3	3.48 s	-
Met-Glc II					
	1	103.3	CH	4.51 (7.6)	C3 Xyl IV
	2	75.8	CH	3.22 m	-
	3	86.5	CH	2.98 t brd (8.8)	C2,C4,C5, OCH_3
	4	69.9	CH	3.19 m	-
	5	79.4	CH	3.41 m brd	-
	6	65.7	CH_2	3.85 m	-
	OCH_3	60.4	CH_3	3.48 s	C3

*Recorded at 400 MHz in DMSO-d6. s (singlet); d (doublet); dd (doublet of doublet), t (triplet); m (multiplet), brd (broad)

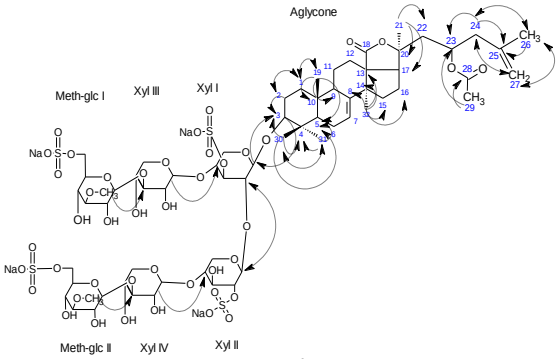

Figure 11: Selected key HMBC correlations of compound C

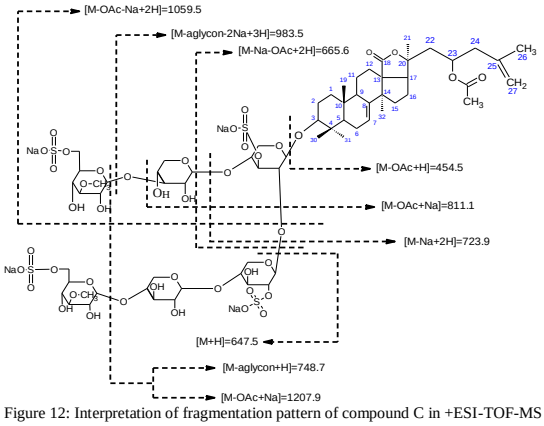

Figure 12: Interpretation of fragmentation pattern of compound C in +ESI-TOF-MS

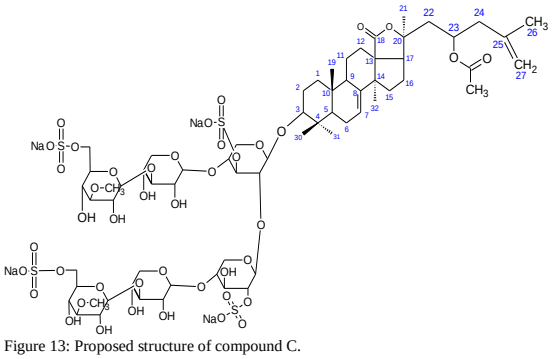

Figure 13: Proposed structure of compound C.

Cytotoxic Effects of the Isolated Compounds

The cytotoxic effects of three compounds (A, B and C) isolated from Malaysian sea cucumber, *S. chloronotus* were evaluated against multiple cell lines including human non-small lung carcinoma (A549), human cervical cancer (C33A), human breast adenocarcinoma (MCF-7), human esophageal carcinoma (TE1), in addition to normal human dermal fibroblasts (NHDF). Curves of percentage cells viability were plotted against the compounds concentrations and presented in Figure 14-16, illustrating the concentration dependent cytotoxic effects of the compounds against each of the cell lines. In addition, the effects of the compounds treatments were compared with that of the positive control, Taxol, as well as the vehicle treatment as a negative control. Approximate inhibitory compound concentrations required to reduce 50% of cell viability were determined base on the concentration-dependent cytotoxicity curves and the values were presented in Table 10.

As shown in Figures 14-16, three compounds exhibited concentration-dependent cytotoxic effects against cancer cells as well as the normal cells (NHDF). However, there was a variation in the activity of the tested compounds against the treated cells. Compound C showed the strongest cytotoxic activity among the three isolated glycosides against MCF-7 (IC_{50}= 2.4 µM), A549 (IC_{50}= 0.9 µM), and NHDF (IC_{50}= 2.0 µM). Whereas compound B exhibited higher cytotoxic effects against both C33A (IC_{50}= 1.3 µM) and TE1 (IC_{50}= 2.2 µM). On the other hand, compound A demonstrated lower cytotoxic effects compared to the other isolated glycosides as well as the positive control, giving IC_{50} range (2.4-7.5 µM) (Table 10).

A549 cells were found to be the most sensitive cells toward the compounds A, C and Taxol, showing IC_{50}= 2.4, 0.9 and 0.8 µM, respectively. While C33A cells showed higher sensitivity toward compound B, giving IC_{50}= 1.3 µM. The positive control (Taxol) exhibited more cytotoxic effects than the isolated glycosides against MCF-7, A549, and C33A cancer cells giving IC_{50} equal to 1.2, 0.8, and 1.9, respectively. On the other hand, the three isolated glycosides demonstrated more cytotoxic effects than Taxol, against both the cancer cells TE1 and the normal cells NHDF cell.

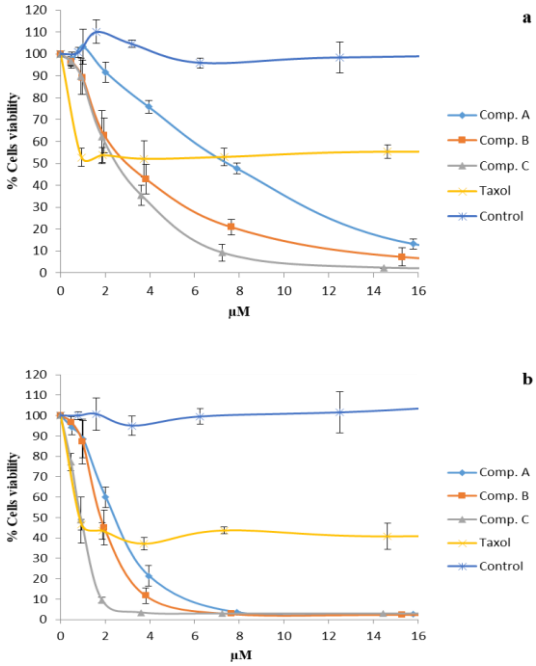

Figure 14: Concentration-dependent effects of *S. chloronotus* glycosides on viability of MCF-7 cells (a), and A549 cells (b). Data were represented by mean values ± SD (n=3).

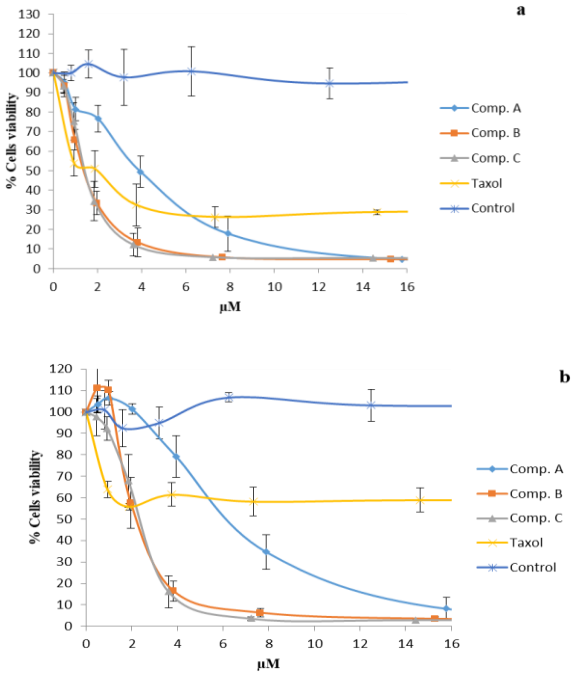

Figure 15: Concentration-dependent effects of *S. chloronotus* glycosides on viability of C33A cells (a), and TE1 cells (b). Data were represented by mean values ± SD (n=3).

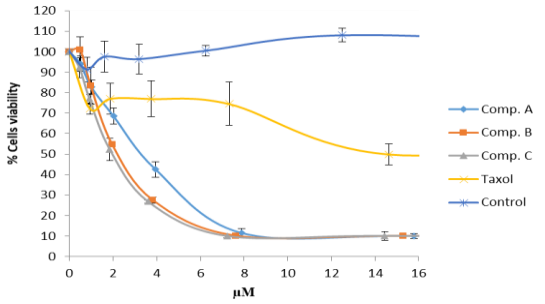

Figure 16: Concentration-dependent effects of *S. chloronotus* glycosides on viability of NHDF cells. Data were represented by mean values ± SD (n=3).

Table 10: Cytotoxic effect of *S. chloronotus* glycosides (A, B, and C) against various cancer cell lines

Compounds	MCF-7	A549	C33A	TE1	NHDF
A	7.5 ± 1.0*	2.4 ± 0.4*	3.9 ± 0.3*	6.0 ± 0.2*	3.5 ± 0.6*
B	2.9 ± 0.7*	1.7 ± 0.2*	1.3 ± 0.2*	2.2 ± 0.2*	2.2 ± 0.6*
C	2.4 ± 0.5*	0.9 ± 0.1	1.4 ± 0.1*	2.3 ± 0.2*	2.0 ± 0.5*
Taxol	1.2 ± 0.1	0.8 ± 0.1	1.9 ± 0.1	ND	15.8 ± 0.6

Data expressed as IC_{50}, the inhibitory concentrations in (µmol/L) required to reduce 50% of cell viability (mean ± SD, n = 3). * Significant difference compared to Taxol IC_{50} at $p < 0.05$ (t-test). ND, Not Determined.

DISCUSSION

Although the crude extracts of natural products have been used since ancient times for treatment of various diseases, the modern pharmaceutical uses of natural products depend mainly on the isolation of a single compound that possess the pharmacological activity (Chaachouay & Zidane, 2024; Najmi et al., 2022; Thomford et al., 2018). Furthermore, identifying structure of the active compounds is essential for drug development and formulation process. Understanding the structure-activity relationship (SAR) is needed for applying the structural modification in order to optimize a therapeutic index, i.e. maximizing the advantageous activity while minimizing the side effects of the pharmaceutical materials (Son et al., 2024; Z. Wang et al., 2023).

Crude extracts usually contain large number of primary and secondary metabolites that posse various chemical and biological properties. Thus, isolation of a single compound exhibiting a desirable pharmaceutical effect from this complex mixture is a kind of complicated task, especially when the chemical nature of the target compound is not known (Simoben et al., 2023). However, implementing of advanced chromatographic techniques as well as following a systematic strategy in the isolation process may help in reducing the efforts and time needed for the isolation process. In fact, choosing a proper isolation technique depends mainly on the physical and chemical characteristics of the active compounds, particularly their lipophilic or hydrophilic properties and molecular size (Shakoor et al., 2023). However, in some cases, as in the case of the present study, the isolation process is started without enough information about the chemical and physical nature of the target compounds, requiring performing a multiple broad and specific separation techniques in a systematic way, in which the isolation process could be guided by the biological activity (Berlinck et al., 2022; Najmi et al., 2022).

A bioactivity-guided isolation method is one of the most successful strategies that has been strongly recommended by several experts in isolation of active compounds from marine organisms (Aggarwal et al., 2022; Banday et al., 2024; Riguera, 1998). This strategy was applied in the present study to isolate the active cytotoxic compounds from sea cucumber, *S. chloronotus.* To achieve this goal, a freeze-dried sample was extracted by absolute methanol, which is described as a polar organic solvent that dissolves a wide range of both hydrophilic and lipophilic compounds. After solvent evaporation, a broad separation of a mixture was performed by successive fractionation between different ratios of hydro-alcoholic solvents with immiscible organic solvents including hexane, carbon tetrachloride, dichloromethane, and finally between butanol and water.

In this study, the polar constituents (water and butanol fractions) were found to represent 84.0% of the recovered extract components while the non-polar constituents (hexane, carbon tetrachloride, and dichloromethane fractions) made up to 16.0% in total. By applying the above liquid-liquid extraction process, it was expected that the high polar organic materials such as alkaloid salts, amino acids, polyhydroxysteroids, etc would be concentrated in the water soluble fraction, while the butanol fraction was composed mainly of saponins contents. Organic compounds with medium polarity, such as peptides and depsipeptides would be concentrated in the dichloromethane fraction. On the other hand hexane and carbon trtrachloride afford only low polarity metabolites including hydrocarbons, fatty acids, acetogenins, and terpenes (Ceesay et al., 2019; Riguera, 1998).

Further subjecting each of the above fractions to MTT assay, the cytotoxic components were found to be concentrated particularly in the butanol fraction. This indicated that the initial separation step has successfully separated the *S. chloronotus* extract components according to their polarities, in which the target cytotoxic compounds were allocated among polar constituents in butanol fraction. Since butanol fraction was expected to contain saponin components, the Liebermann-Burchard test was applied to confirm the presence of saponin in this fraction which gave positive result. In fact, many of saponins (triterpene glycone resuides) that have been isolated from various sea cucumber species showed significant cytotoxic activities. Accordingly, it was hypothesized that the active cytotoxic compounds present in the butanol fraction of *S. chloronotus* are saponins, most probably triterpene glycosides.

Since the active cytotoxic compounds were found in the high polar fraction, the further step of the isolation process aimed to get rid of the inorganic salts that might be found in a significant amount in this fraction. Removing of these salts is very important as they might interfere with the biological assays as well as chromatographic separation methods (Bhakuni & Rawat, 2005; Tang et al., 2022). For this purpose, the method recommended by Shimizu and Li was followed (Shimizu & Li, 2008). Hence, the removing of the inorganic salts was achieved after retention of the organic components on a nonionic resin (Amberlite XAD-2), and then the mineral salts were eluted first with water, followed by eluting of the organic constituents with methanol.

The second broad separation method was achieved through vacuum liquid chromatography by using a gradient elution with mobile phase of chloroform and methanol. By the aid of this technique the small amounts of medium and less polar components were eluted with mobile phases containing high chloroform concentration (>70%), while the more polar compounds, representing the majority of fraction components, were eluted together with lower chloroform and higher methanol concentrations. Subjecting of the obtained fractions to the MTT assay showed that the active cytotoxic compounds were concentrated again in the high polarity components, supporting the above hypothesis that the active cytotoxic components could possibly be triterpene glycosides.

The combined active subfractions were then separated according to their molecular sizes by gel filtration method using Sephadex LH-20 to yield an active cytotoxic fraction containing three compounds A, B and C as demonstrated on TLC. After partial isolation of the compounds A, B and C through normal phase column chromatography, the final purification of each compound was achieved by using reverse phase column chromatography. It is well known that the reverse phase chromatography is the ideal method for isolation of high polarity compounds. However, using a reverse phase column is encountered with a limited sample size, because injection of large amounts of the crude material could result in the incapacitation of a column (Bhakuni & Rawat, 2005; Miller & Ayube, 2020). For this reason, the isolation on reverse-phase columns was performed only for the fine separation at the final purification step.

The purities of the isolated compounds were confirmed by using TLC as well as HPLC methods. The normal phase TLC plate coated with silica gel interacts with polar function groups and thus adsorbs the very polar compounds for a longer period compared to those with relatively lower polarities. On the other hand, in case of the reverse phase TLC plate as well as HPLC column, the stationary phases were composed of silica gel attached to C18 hydrocarbon chain that preferably adsorbs the less polar compounds rather than the more polar compounds. Accordingly, compound A, which is relatively less polar than the compounds B and C, was eluted first in the normal phase chromatography (R_f = 0.2), subsequently followed by B and C (R_f = 0.17, and 0.1). In contrast, the highest polar isolated compound (C) was eluted first from the reverse phase chromatography using TLC and HPLC (R_f = 0.4, R_t = 4.08 min.), which was followed by compound B (R_f = 0.33, R_t = 4.65 min.), and lastly compound A (R_f = 0.25, R_t = 5.68 min.).

After the active compounds were isolated, the efforts were concentrated on the structural elucidation of these compounds. In the first step of the structural identification process a Liebermann-Burchard test was performed to prove the hypothesis that the isolated active compounds are saponins. The three active compounds demonstrated positive reaction with Liebermann-Burchard reagent indicating the presence of triterpenes (more often) or steroids (seldom) moieties in their structures. Furthermore, the final structures of the isolated compounds were elucidated with the aid of an extensive spectroscopic analysis by using IR, ^{13}C and ^{1}H- NMR (1D and 2D), in addition to ESI-TOF-MS spectra. In fact, the structural identification progression in the present study has been assisted efficiently by reviewing the previous studies that have isolated triterpene glycosides (saponins) from various sea cucumber species (Han et al., 2009; Kitagawa, Kobayashi, Inamoto, Yasuzawa, & Kyogoku, 1981; Silchenko et al., 2008; X. Wang et al., 2022; W.-S. Yang et al., 2021; Zhang et al., 2006; Zou et al., 2003).

Among all of the spectroscopic methods, obtaining and interpretating IR absorption spectrum is considered the fastest and easiest method. IR spectrum emphasizes the information on determining the existence of some functional groups, especially the strong polar functional groups such as hydroxyl, amino, and carbonyl groups (Nandiyanto et al., 2023; Ning, 2011). Based on the IR spectra of the isolated saponins, they were primarily identified as triterpene glycosides containing γ-lactone; a five-membered ring in which carbon of carbonyl group and an adjacent oxygen form part of the ring; and an acetyl group which was indicated by a broad band at 1735 cm^{-1}. In addition to the γ-lactone band, strong broad absorptions at 3405 cm^{-1} suggested a triterpene glycosidic structure (Silchenko et al., 2024; Zhang et al., 2006). Additional valuable information concluded from the IR spectra of the isolated compounds was the presence of sulphate group, which was indicated by absorption bands at 1245 and 1071 cm^{-1}.

As was elaborated previously in the results section, the structures of the three isolated triterpene glycosides were identified with the aid of the comprehensive 1D and 2D ^{1}H and ^{13}C-NMR and ESI-TOF-MS spectra. HMQC experiment correlated all proton resonances with those of their corresponding carbons in the carbohydrates and aglycone moieties. Starting from the easily distinguished signals, like those of the proton on the carbons involved in double bonds and anomeric protons of the sugar units, COSY experiment allowed the sequential assignment of most of the resonances for aglycone and sugar rings. By the HMBC experiment, the location of the function groups as well as the interglycosidic linkages between sugar –sugar and sugar-aglycone was deduced. As shown in the results section, the signals of the carbons involved in the glycosidic linkages, like C2 of the first xylose in the three compounds δ_C 82.7, were shifted downfield relative to shifts expected for the corresponding methyl glycopyranosides. Moreover, the complexity of the NMR data, produced by 66 carbons and their corresponding protons in each compound, was solved when the spectra were matched with those of previously isolated triterpene glycosides from *S. chloronotus* and other sea cucumber species.

The confirmation of the final structures was performed after indicating the molecular weight and the fragmentation pattern of each compound by using ESI-TOF-MS spectra. Mass spectrometry (MS) provides very valuable information for the structural elucidation of unknown compounds. However, MS of the compounds found in the more polar fractions like saponins are better taken under soft ionization techniques such as chemical ionization (CI), fast atom bombardment (FAB), matrix assisted laser desorption-ionization (MALDI), and electrospay ionization (ESI) (Ning, 2011). Van Dyck et al. (2009) implemented two mass spectrometry techniques (MALDI- and ESI-MS) to highlight remarkable differences between the saponin mixtures of *Holothuria forskali*. A total of 36 different structures of triterpene glycosides including many isomer congeners were detected in the body wall and cuvierian tubules of *H. forskali* by aid of these soft ionization MS techniques (Van Dyck et al., 2009). In another study, the same research group used these MS techniques in analyzing qualitative and quantitative saponin contents in five sea cucumber species from the Indian Ocean (Van Dyck et al., 2010).

In the present study, after interpretation of the spectra obtained from each of the above spectroscopic techniques, the structure of glycoside A was identified as holostane triterpenoid containing a double bond (Δ^7) and attached to acetoxy group at C23 in addition to hexasaccharide chain at C3. The hexasaccharide units are branched at the first sulphated xylose unit to give another xylose unit and 3-*O*-methyl xylose at the branch end, while the second branch contains quinovose, xylose and 3-*O*-methyl glucose, sequentially. Glycoside B contains the same holostane triterpenoid but a different carbohydrate chain, which is composed of sulphated xylose unit, branched to a chain of xylose and sulphated 3-*O*-methyl glucose in the first branch and to a sequence of xylose-xylose-sulphated 3-*O*-methyl glucose in the second branch. On the other hand, compound C was identified as a glycoside having the same holostane triterpenoid. The deferences between glycosides C and B are ascribed to the presence of an additional double bond (Δ^{25}) in the aglycone structure and the presence of an additional sulphate group attached to xylose II sugar unit of glycoside C.

On the basis of the data discussed above, the structure of glycoside A was determined to be 3β-*O*-{[6-*O*- sodium sulphate-3-*O*-methyl- β -D-gluco- pyranosyl-(1→3)- β -D-xylopyranosyl-(1→4)- β -D-quinovopyranosyl-(1→2)]-[O-(3-*O*-methyl- β D-xylopyranosyl -(1→3)- β -D-xylopyranosyl-(1→4)]-3- *O*- sodium sulphate-β -D- xylopyranosyl}-23-acetoxyholosta-7-ene. The structure of compound B was identified as 3β-*O*-{[6-*O*- sodium sulphate-3-*O*-methyl- β -D-gluco- pyranosyl-(1→3)- β -D-xylopyranosyl-(1→4)- β -D-xylopyranosyl-(1→2)]-[6-*O*- sodium sulphate-3-*O*-methyl- β -D-gluco- pyranosyl -(1→3)- β -D-xylopyranosyl-(1→4)]-3- *O*- sodium sulphate-β -D- xylopyranosyl}-23-acetoxyholosta-7-ene, and as for the compound C, the structure was defined as 3β-*O*-{[6-*O*- sodium sulphate-3-*O*-methyl- β -D-gluco- pyranosyl-(1→3)- β -D-xylopyranosyl-(1→4)- 3-*O*- sodium sulphate- β -D-xylopyranosyl-(1→2)]-[6-*O*- sodium sulphate-3-*O*-methyl- β -D-gluco- pyranosyl -(1→3)- β -D-xylopyranosyl-(1→4)]-3- *O*- sodium sulphate-β -D- xylopyranosyl}-23-acetoxyholosta7,25-diene.

Although saponins, including triterpene glycosides, are very common in plants, for animals they are found only in some marine invertebrates such as sea cucumbers, sea stars, and sponges. Indeed, the presence of triterpene glycoside saponins is characteristic for most sea cucumber species (Fagbohun et al., 2023; Khodja et al., 2024; Mondol et al., 2017). Generally, sea cucumber saponin structures are made up of a sugar chain (glycone) linked to the C-3 of the triterpenoid aglycone, so called triterpene glycoside. Aglycone structures of sea cucumber glycosides are based on a lanosterol-type triterpene with a distinctive D-ring with fused 18(20)-γ-lactone skeleton named holostane. On the other hand, the carbohydrate chains contain only xylose, quinovose, glucose, 3-*O*-methylglucose, and rarely 3-*O*-methylxylose, in which xylose is always the first monosaccharide unit attached to C3 of a triterpene aglycone, while a methylated sugar (3-*O*-methylglucose or 3-*O*-methylxylose) is always the terminal residue. Many glycosides

have been found to contain sulphate groups at C-4 of the first xylose and at C-6 of glucose and *3-O*-methylglucose residues (Silchenko et al., 2020, 2021).

The isolated glycosides in this study had the distinguished carbohydrate parts compared with stichoposides A1 (33), A2 (34), B1 (35), B2 (36), C1 (37) and C2 (38) which were isolated twenty years ago from *S. chloronotus* collected from Okinawa in Japan by Kitagawa and co-researchers (Kitagawa, Kobayashi, Inamoto, Yasuzawa, & Kyogoku, 1981; Kitagawa, Kobayashi, Inamoto, Yasuzawa, Kyogoku, et al., 1981), while the aglycones, stichlorogenol and dehydrostichlorogenol, were unchanged. The main differences were the presence of sulphate groups attached to the sugar units of compounds A, B, and C; and the presence of methyl xylose at one terminal of the carbohydrate chain of compound A. On the bases of the early findings by Kitagawa research group (Kitagawa, Kobayashi, Inamoto, Yasuzawa, & Kyogoku, 1981; Kitagawa, Kobayashi, Inamoto, Yasuzawa, Kyogoku, et al., 1981), the glycosides of genous *Stichopus* have been distinguished by the lack of sulphate groups. However, the present study concluded the presence of the sulphate groups in *S. chloronotus* glycosides by the aid of IR and ESI-TOF-MS spectra, which were not used by Kitagawa research group. It is well known that C13 NMR spectrum does not show characteristic signals for the attachement of sulphate group. On the other hand, Moraes and colleagues (2004) have implemented 1D NMR (^{13}C, DEPT, ^{1}H) and 2D NMR (^{1}H-^{1}H COSY, NOESY, HSQC, HMBC) spectra and MALDI-TOF-MS to elucidate the structure of sulphated glycosides, neothyonidioside, mollisosides A, B1, and B2 from *Stichopus mollis.* After identification of these sulphated glycosides, the taxonomic status *Stichopus mollis* was revised and placed into a new genus, *Australostichopus* (Moraes et al., 2004).

It is interesting to note that while Kitagawa et al. (1981) have isolated both stichlorogenol and dehydrostichlorogenol containing glycosides from *S. chloronotus* collected from the Japanese coast- (Kitagawa, Nishino, et al., 1981). Maltsev et al. (1983) found only dehydrostichlorogenol derivatives in specemen of the same species collected from the Great Barrier Reef (Mal'tsev et al., 1983). Moreover, Maltsev et al. (1984) isolated triterpene glycosides (holotoxins) from *Stichopus japonicus* collected from Posiet Bay, Japan Sea, having different carbohydrate moieties from those of holotoxins A and B isolated from the same species collected near the Japan shore by Kitagawa research group (Kitagawa et al., 1978; Maltsev et al., 1984). It was supposed that the carbohydrate ingredients in the *Stichopus japonicus* sugar moieties are able to vary if the habitat of the animal differs (Kitagawa et al., 1978). This is one of the possible reasons for the observed distinctions of *S. chloronotus* glycosides isolated in the present study.

Moreover, during these years, and by the aid of using the sensitive spectroscopic instumentations, many glycosides with uncommon structural features were identified. For examples, the presence of quinovose as terminal monosaccharide unit and the presence of two quinovose residues; the presence of glucose instead of common xylose as fifth terminal monosaccharide unit; trisaccharide carbohydrate chain; the presence of two 3- O-methylxylose terminal monosaccharide units; and the presence of sulphate group at C-3 of quinovose residue. Furthermore, 17α- and 12α-hydroxyls, which are characteristic for glycosides from sea cucumbers belonging to the family Holothuriidae (order Aspidoschirotida), was interestingly identified in some aglycones of glycosides from representatives of the order Dendrochirotida confirming the parallel and independent character of evolution of glycosides (Kalinin et al., 2005).

Sea cucumber triterpene glycosides have attracted interests for their pharmacological and ecological values. So far, more than 300 different structures of triterpene glycosides have been isolated from various sea cucumber species (Mondol et al., 2017). These secondary metabolites have exhibited a wide spectrum of biological activities including hemolytic, imunomodulatory, anti-inflammatory, antifungal, antibacterial, antiviral, antitumour, cytostatic and antineoplastic properties (Kalinin et al., 2021; Sanjeewa & Herath, 2023).

The present study emphasized on the cytotoxic activity of *S. chloronotus* triterpene glycosides. The three isolated glycosides A, B, and C exhibited potent cytotoxic activities against four solid tumour cell lines which are human non-small lung carcinoma (A549), human cervical cancer (C33A), human breast adenocarcinoma (MCF-7), human esophageal carcinoma (TE1), and one type of normal cells i.e. normal human dermal fibroblasts (NHDF). Like most of the other biological activities exhibited by saponins, their cytotoxic effect seems to result from their ability to bind with cell membrane cholesterol causing membranotropic effects. The mebranotropic effect was also found to be linked to their surfactant and amphiphilic nature which results from the presence of a hydrophilic sugar moiety and a hydrophobic aglycone (Gaudin et al., 2019; Gauthier et al., 2009; Timilsena et al., 2023). Furthermore, saponin structures affect the environment surrounding the cell membrane by alterating the negatively charged carbohydrate portions on the cell surface, causing changes in the transmembrane signals (Torres et al., 2021).

Each of the isolated glycoside and the standard drug (Taxol) showed variable cytotoxic potencies against the various treated cells. Compound A was found to be more selective to A549 cells (IC_{50} = 3.8 µg/ml), while B showed the maximum cytotoxic activity against C33A (IC_{50} = 2.2 µg/ml). On the other hand, glycoside C was found to be the most potent amongst the isolated glycosides, exhibiting its maximum cytotoxic activity against A549 (IC_{50} = 1.5 µg/ml). Similar to glycosides A and C, Taxol demonstrated its most cytotoxic effect against A549 cells. However, MCF-7 was found to be the most resistant cell line towards the glycoside treatment, while TE1 was found to be resistant to Taxol treatment. All of the isolated compounds and Taxol drug demonstrated levels of cytotoxic actions against the normal cells (NHDF) which showed higher sensitivity to the glycoside treatments (IC_{50} = 2.0-3.5 µg/ml) than Taxol (IC_{50} = 15.8 µg/ml).

The cytotoxic effects of triterpene glycosides fractions from *Stichopus chloronotus* and *Thelenota ananas* against lymphocyte leukemia P-388 were demonstrated earely by (Pettit, G. et al., 1976). In addition, stichoposides A, C, D and E affected survival of Ehrlich tumour cells with minimal effective concentrations ranged from 3.1 to 12 µg/ml. Stichoposide A, with two monosaccharide units, and stichoposide E, with the xylose residue as second monosaccharide unit, were less active than Stichoposide C, a quinovose-containing hexaoside (Kalinin et al., 2008). The action of triterpene glycosides from sea cucumbers on early embryogenesis of sea urchins is related to their membranotrobic and cytotoxic effects. Thus, the inhibitory effects of *Stichopus* glycosides, Stichoposide A, C, D and E, on the division of fertilized eggs of the sea urchin *Strongylocentrotus intermedius* were reported recently by Kalinin et al. (2008). Stichoposide C, was found to be the most active one, while stichoposides D and E having no a quinovose residue showed lower activity than stichoposide C.

Interactions of saponins with cell membranes and thus their cytotoxic activities are varied with respect to saponin structure as well as the cell membrane characteristics (Podolak et al., 2023). In fact, the cytotoxic activities of saponins are strongly related to the structures of both the aglycone part and the carbohydrate chain. The presence of an 18(20)-lactone and at least one oxygen group near it has critical significance for biological activity of sea cucumber glycosides. The glycosides with a 7(8)-double bond but not a 16-ketogroup were found to be more active than those having 9(11)-double bond (Elmaidomy et al., 2023; Kalinin et al., 1996). Moreover, It has been concluded that the presence of acetyl group at C-16 of the aglycone in frondoside A was the structural feature responsible for an increased cytotoxicity and apoptosis induction by this glycoside, comparing to cucumariosides A2-2 in which the acetyl group is replaced by keto group (Jin et al., 2009; Park et al., 2014).

In the carbohydrate moiety, a linear tetrasaccharide fragment is also significant for membranotropic action (Zelepuga et al., 2021). It has been found that the glycosides having quinovose as a second monosaccharide unit are more active than those with xylose or glucose unit (Silchenko et al., 2024). On the contrary,

the present study showed compound A, having quinovose, is less active than B and C which contain xylose units. This might refer to the presence of other structural varioations such as the number of sulphate groups attached to sugar moieties. Kalinin et al. (1996) reported that presence of a sulphate group at C-6 of the third monosaccharide unit increases K^+ loss from erythrocyte membranes. A sulphate at C-4 of the first xylose of nonbranched glycosides having a linear tetrasaccharide unit does not significantly affect activity but its absence in biosides decreases their activity (Kalinin et al., 1996; Mondol et al., 2017). However, in case of the present study, the three glycosides are distinguished by the presence of branched hexosides carbohydrate moieties. Moreover, the sulphate group at xylose1 was found to be the key functional group required for the immunomodulatory effects of cucumariosides A2-2 and A4-2 (Aminin et al., 2001; Pradhan et al., 2023). Thus, the higher cytotoxic effects demonstrated by compound C might be also related to the additional sulphate groups present on its carbohydrate moieties.

Valuable data could be gained from the observations of the studies emphasized on SAR with regard to cytotoxicity of plant saponins. A very helpful review, that discussed the correlations between the molecular structure and the cytotoxicity of both steroid and triterpenoid saponins as well as the most common mechanisms of action, was recently prepared by Podolak and co-authors (Podolak et al., 2010). The authors have concluded that for all saponins both the aglycone and sugar parts play an important role for cytotoxic activity. Regarding the aglycone part, the main structural features related to the enhanced cytotoxicity were described as free carboxyl at C-28, free hydroxyl at C-16 and acylation at C16, C21, C22, C25, and C28 (Jin et al., 2009; Podolak et al., 2023). In contrast, it was postulated that the presence of hydroxyl group at C-23 has a detrimental effect on the cytotoxic potential of tested saponins (Sobolewska et al., 2020).

Moreover, the cytotoxic activities of natural triterpene glycosides have been affected by the numbers, types, and even the sequences of carbohydrate chain. For example, the presence of α-L-arabinopyranosyl as the first sugar attached at C-3, especially in a sequence of α-L-Rhap-(1-2)-α-L-Arap, is a structural requirement essential for potent cytotoxic activity of oleanane saponins. It was observed that saponins having a non-natural anomeric configuration of β-L- or α-D were inactive or only slightly active. The presence of β-D-glucosepyranosyl either at C-3 or C-28 has a negative effect on the cytotoxicity of lupane-type saponins (Bildziukevich et al., 2023).

Accordingly, it could be postulated that the variation in the cytotoxic activities of the isolated triterpene glycosides in this study is related to the structural variation of aglycones as well as carbohydrate chains. As far as the aglycones are concerned, the presence of an additional double bond (Δ^{25}) is the only distinctive structural feature that might be responsible for the enhanced cytotoxic activity of compound C. The variations in the potential of cytotoxic activities of the isolated compounds might be resulted from the replacement of quinovose with xylose residue and the presence of additional sulphate groups in the carbohydrate moieties. However, with such extreme shortage in scientific data about the structur-activity relationship in regard to cytotoxicity of sea cucumber triterpene glycosides, it is very difficult to generalize these explanations; and it may be subjected to bias. Thus, it is strongly recommended to conduct a comprehensive study in this respect.

CONCLUSION

It could be concluded that the cytotoxic activity demonstrated by the crude extract of *S. chloronotus* is related to the presence of saponin triterpene glycosides. Three major cytotoxic compounds (A, B, and C) were isolated from the butanol fraction and were further identified as holostane type triterpene glycosides. The three isolated glycosides exhibited various levels of cytotoxic potentials against four cancer cell lines as well as one type of normal cells, where compound C showed the most potent effect, followed by compound B, and then compound A. Studying the cytotoxic activity in relation to the structural variations suggested that both aglycone and carbohydrate moieties of the isolated glycosides contributed to their cytotoxic effects. Presence of the additional double bond Δ^{25} as well as the sulphate groups might contribute to the superior cytotoxicity of compound C. Further study is needed to identify the mechanism of cell death induced by the isolated glycosides in the hope of finding a new approach that may overcome the multi drug resistant mechanisms in cancer cells.

Funding Sources

This study was not supported by any sponsor or funder.

Data Availability

The original contributions presented in the study are included in the article/Supplementary material, further inquiries can be directed to the corresponding authors.

Conflict of Interest Statement

The authors have no conflicts of interest to declare.

References

Aggarwal, M., Singh, R., Ahlawat, P., and Singh, K. (2022). Bioactive Extracts: Strategies to Generate Diversified Natural Product-Like Libraries. *Current Bioactive Compounds*, **18**(9), 30–49. https://doi.org/10.2174/1573407218666220111105443

Althunibat, O. Y., Hashim, R. Bin, Taher, M., Daud, J. M., Ikeda, M.-A., and Zali, B. I. (2009). In vitro antioxidant and antiproliferative activities of three Malaysian sea cucumber species. *Eur J Sci Res*, **37**(3), 376–387.

Aminin, D. L., Agafonova, I. G., Berdyshev, E. V, Isachenko, E. G., Avilov, S. A., and Stonik, V. A. (2001). Immunomodulatory Properties of Cucumariosides from the Edible Far-Eastern Holothurian Cucumaria japonica. *Journal of Medicinal Food*, **4**(3), 127–135. https://doi.org/10.1089/109662001753165701

Banday, A. H., Azha, N. ul, Farooq, R., Sheikh, S. A., Ganie, M. A., Parray, M. N., Mushtaq, H., Hameed, I., and Lone, M. A. (2024). Exploring the potential of marine natural products in drug development: A comprehensive review. *Phytochemistry Letters*, **59**, 124–135. https://doi.org/10.1016/j.phytol.2024.01.001

Berlinck, R. G. S., Crnkovic, C. M., Gubiani, J. R., Bernardi, D. I., Ióca, L. P., and Quintana-Bulla, J. I. (2022). The isolation of water-soluble natural products – challenges, strategies and perspectives. *Natural Product Reports*, **39**(3), 596–669. https://doi.org/10.1039/D1NP00037C

Bhakuni, D. S., and Rawat, D. (2005). Bioactive Marine Natural Products. *Bioactive Marine Natural Products*, 1–382. https://doi.org/10.1007/1-4020-3484-9

Bildziukevich, U., Wimmerová, M., and Wimmer, Z. (2023). Saponins of Selected Triterpenoids as Potential Therapeutic Agents: A Review. *Pharmaceuticals*, **16**(3), 386. https://doi.org/10.3390/ph16030386

Bordbar, S., Anwar, F., and Saari, N. (2011). High-Value Components and Bioactives from Sea Cucumbers for Functional Foods—A Review. *Marine Drugs*, **9**(10), 1761–1805. https://doi.org/10.3390/md9101761

Ceesay, A., Nor Shamsudin, M., Aliyu-Paiko, M., Ismail, I. S., Nazarudin, M. F., and Mohamed Alipiah, N. (2019). Extraction and Characterization of Organ Components of the Malaysian Sea Cucumber Holothuria leucospilota Yielded Bioactives Exhibiting Diverse Properties. *BioMed Research International*, **2019**(1), 2640684. https://doi.org/10.1155/2019/2640684

Chaachouay, N., and Zidane, L. (2024). Plant-Derived Natural Products: A Source for Drug Discovery and Development. *Drugs and Drug Candidates*, **3**(1), 184–207. https://doi.org/10.3390/ddc3010011

Coelho, F. P., and Alves, F. A. (1946). Liebermann-Burchard Reaction. *Nature*, **157**(3998), 803. https://doi.org/10.1038/157803a0

CONAND, C., UTHICKE, S., and HOAREAU, T. (2002). Sexual and asexual reproduction of the holothurian Stichopus chloronotus (Echinodermata): a comparison between La Réunion (Indian Ocean) and east Australia (Pacific Ocean). *Invertebrate Reproduction & Development*, **41**(1–3), 235–242. https://doi.org/10.1080/07924259.2002.9652756

Cuc, N. T., Nga, N. T., Phuong, T. H., Cuong, N. X., Huong, P. T. M., and Van Minh, C. (2020). The anticancer activities of stichoposide D isolated from the sea cucumber Stichopus chloronotus on NTERA-2 cancer stem cells. *Journal of Biotechnology*, **18**(2), 273–281. https://doi.org/10.15625/1811-4989/18/2/14375

Ding, X., Collin, P., Witt, R., Talamonti, M., Bell, R., and Adrian, T. E. (2004). Myristoleic acid, isolated from the oil of the sea Cucumber Cucumaria frondosa, inhibits proliferation of human pancreatic cancer cells in vivo and in vitro. *The Journal of Nutrition*, **134**(12S), 3528S-3528S.

Elmaidomy, A. H., El Zawily, A., Salem, A. K., Altemani, F. H., Algehainy, N. A., Altemani, A. H., Rateb, M. E., Abdelmohsen, U. R., and Shady, N. H. (2023). New cytotoxic dammarane type saponins from Ziziphus spina-christi. *Scientific Reports*, **13**(1), 20612. https://doi.org/10.1038/s41598-023-46841-2

Fagbohun, O. F., Joseph, J. S., Oriyomi, O. V, and Rupasinghe, H. P. V. (2023). Saponins of North Atlantic Sea Cucumber: Chemistry, Health Benefits, and Future Prospectives. *Marine Drugs*, **21**(5), 262. https://doi.org/10.3390/md21050262

Fredalina, B. D., Ridzwan, B. H., Abidin, A. A. Z., Kaswandi, M. A., Zaiton, H., Zali, I., Kittakoop, P., and Jais, A. M. M. (1999). Fatty acid compositions in local sea cucumber,. *General Pharmacology: The Vascular System*, **33**(4), 337–340. https://doi.org/10.1016/S0306-3623(98)00253-5

Gaudin, T., Lu, H., Fayet, G., Berthauld-Drelich, A., Rotureau, P., Pourceau, G., Wadouachi, A., Van Hecke, E., Nesterenko, A., and Pezron, I. (2019). Impact of the chemical structure on amphiphilic properties of sugar-based surfactants: A literature overview. *Advances in Colloid and Interface Science*, **270**, 87–100. https://doi.org/https://doi.org/10.1016/j.cis.2019.06.003

Gauthier, C., Legault, J., Girard-Lalancette, K., Mshvildadze, V., and Pichette, A. (2009). Haemolytic activity, cytotoxicity and membrane cell

permeabilization of semi-synthetic and natural lupane- and oleanane-type saponins. *Bioorganic & Medicinal Chemistry*, **17**(5), 2002–2008. https://doi.org/10.1016/j.bmc.2009.01.022

Han, H., Yi, Y., Li, L., Wang, X., and Pan, M. (2012). Triterpene Glycosides from Sea Cucumber Holothuria scabra with Cytotoxic Activity. *Chinese Herbal Medicines*, **4**(3), 183–188. https://doi.org/10.3969/j.issn.1674-6384.2012.03.002

Han, H., Yi, Y., Xu, Q., La, M., and Zhang, H. (2009). Two new cytotoxic triterpene glycosides from the sea cucumber Holothuria scabra. *Planta Medica*, **75**(15), 1608–1612. https://doi.org/10.1055/s-0029-1185865

Hing, H. L., Ambia, K. M., Azraul-Mumtazah, R., Hamidah, S. A., Sahalan, A. Z., Shamsudin, N., Shamsudin, M. W., and Hashim, R. (2007). Effect of Methanol Extracts from Sea Cucumbers Holothuria edulis and Stichopus chloronotus on Candida albicans. *Microscopy and Microanalysis*, **13**(S02), 270–271. https://doi.org/DOI: 10.1017/S1431927607071553

Hossain, A., Dave, D., and Shahidi, F. (2023). Sulfated polysaccharides in sea cucumbers and their biological properties: A review. *International Journal of Biological Macromolecules*, **253**, 127329. https://doi.org/10.1016/j.ijbiomac.2023.127329

Jin, J.-O., Shastina, V. V, Shin, S.-W., Xu, Q., Park, J.-I., Rasskazov, V. A., Avilov, S. A., Fedorov, S. N., Stonik, V. A., and Kwak, J.-Y. (2009). Differential effects of triterpene glycosides, frondoside A and cucumarioside A2-2 isolated from sea cucumbers on caspase activation and apoptosis of human leukemia cells. *FEBS Letters*, **583**(4), 697–702. https://doi.org/10.1016/j.febslet.2009.01.010

Kalinin, V. I., Aminin, D. L., Avilov, S. A., Silchenko, A. S., and Stonik, V. A. (2008). Triterpene Glycosides from Sea Cucucmbers (Holothurioidea, Echinodermata). Biological Activities and Functions. In B. T.-S. in N. P. C. Atta-ur-Rahman (Ed.), *Bioactive Natural Products (Part O)* (Vol. 35, pp. 135–196). Elsevier. https://doi.org/10.1016/S1572-5995(08)80006-3

Kalinin, V. I., Prokofieva, N. G., Likhatskaya, G. N., Schentsova, E. B., Agafonova, I. G., Avilov, S. A., and Drozdova, O. A. (1996). Hemolytic activities of triterpene glycosides from the holothurian order Dendrochirotida: some trends in the evolution of this group of toxins. *Toxicon*, **34**(4), 475–483. https://doi.org/10.1016/0041-0101(95)00142-5

Kalinin, V. I., Silchenko, A. S., Avilov, S. A., and Stonik, V. A. (2021). Progress in the Studies of Triterpene Glycosides From Sea Cucumbers (Holothuroidea, Echinodermata) Between 2017 and 2021. *Natural Product Communications*, **16**(10), 1934578X211053934. https://doi.org/10.1177/1934578X211053934

Kalinin, V. I., Silchenko, A. S., Avilov, S. A., Stonik, V. A., and Smirnov, A. V. (2005). Sea Cucumbers Triterpene Glycosides, the Recent Progress in Structural Elucidation and Chemotaxonomy. *Phytochemistry Reviews*, **4**(2), 221–236. https://doi.org/10.1007/s11101-005-1354-y

Kamarudin, K. R., Rehan, A. M., Hashim, R., and Usup, G. (2010). An update on diversity of sea cucumbers (Echinodermata: Holothuroidea) in Malaysia. *Malayan Nature Journal*, **62**(3), 315–334.

Khodja, I., Mezali, K., Savarino, P., Gerbaux, P., Flammang, P., and Caulier, G. (2024). Structural Characterization and Profiles of Saponins from Two Algerian Sea Cucumbers. *Molecules*, **29**(22), 5346. https://doi.org/10.3390/molecules29225346

Kitagawa, I., Kobayashi, M., Inamoto, T., Yasuzawa, T., and Kyogoku, Y. (1981). The structures of six antifungal oligoglycosides, stichlorosides A1, A2, B1, B2, C1, and C2, from the sea cucumber Stichopus chloronotus (Brandt). *Chemical and Pharmaceutical Bulletin*, **29**(8), 2387–2391.

Kitagawa, I., Kobayashi, M., Inamoto, T., Yasuzawa, T., Kyogoku, Y., and Kido, M. (1981). Stichlorogenol and Dehydrostichlorogenol, Genuine Aglycones of Stichlorosides A1, B1, C1 and A2, B2, C2, from the Sea Cucumber Stichopus chloronotus (Brandt). *Chemical & Pharmaceutical Bulletin*, **29**(8), 1189-1192.

Kitagawa, I., Nishino, T., Kobayashi, M., and Kyogoku, Y. (1981). Marine Natural Products. VIII. Bioactive Triterpene-Oligoglycosides from the Sea Cucumber Holothuria leucospilota BRANDT (2). Structure of Holethurin A. *Chemical & Pharmaceutical Bulletin*, **29**(7), 1951–1956. https://doi.org/10.1248/cpb.29.1951

Kitagawa, I., Yamanaka, H., Kobayashi, M., Nishino, T., Yosioka, I., and Sugawara, T. (1978). Saponin and Sapogenol. XXVII. Revised Structures of Holotoxin A and Holotoxin B, Two Antifungal Oligoglycosides from the Sea Cucumber Stichopus japonicus SELENKA. *Chemical & Pharmaceutical Bulletin*, **26**(12), 3722–3731. https://doi.org/10.1248/cpb.26.3722

Li, R., Mou, J., Zhao, L., Hu, M., Wang, B., Sun, Y., Liu, J., Qi, X., and Yang, J. (2024). Fucoidan from Stichopus chloronotus relieved DSS induced ulcerative colitis through inhibiting intestinal barrier disruption and oxidative stress. *International Journal of Biological Macromolecules*, **283**, 137811. https://doi.org/https://doi.org/10.1016/j.ijbiomac.2024.137811

Mal'tsev, I. I., Stonik, V. A., and Kalinovskii, A. I. (1983). Stichoposide E -A new triterpene glycoside from holothurians of the family Stichopodidae. *Chemistry of Natural Compounds*, **19**(3), 292–295.

Maltsev, I. I., Stonik, V. A., Kalinovsky, A. I., and Elyakov, G. B. (1984). Triterpene glycosides from sea cucumber Stichopus japonicus Selenka. *Comparative Biochemistry and Physiology. B, Comparative Biochemistry*, **78**(2), 421–426. https://doi.org/10.1016/0305-0491(84)90052-x

Maskur, M., Sayuti, M., Widyasari, F., and Setiarto, R. H. B. (2024). Bioactive Compound and Functional Properties of Sea Cucumbers as Nutraceutical Products. *Reviews in Agricultural Science*, **12**, 45–64. https://doi.org/10.7831/ras.12.0_45

Mazlan, N. B., Abd Rahman, N. N. B., Shukhairi, S. S. B., and Nazahuddin, M. N. A. Bin. (2023). *Sea Cucumbers: Source of Nutritional, Medicinal, and Cosmeceutical Products BT - Marine Biotechnology: Applications in Food, Drugs and Energy* (M. D. Shah, J. Ransangan, & B. A. Venmathi Maran (eds.); pp. 171–188). Springer Nature Singapore. https://doi.org/10.1007/978-981-99-0624-6_8

Miller, L., and Ayube, S. J. (2020). In-column dilution: Improving volume loadability in reverse phase gradient chromatography through the use of a silica pre-column. *Journal of Chromatography. A*, **1618**, 460897. https://doi.org/10.1016/j.chroma.2020.460897

Mohd Heikal, M. Y., Ahmad Nazrun, S., Chua, K. H., and Norzana, A. G. (2019). Stichopus chloronotus aqueous extract as a chondroprotective agent for human chondrocytes isolated from osteoarthritis articular cartilage in vitro. *Cytotechnology*, **71**(2), 521–537. https://doi.org/10.1007/s10616-019-00298-2

Mohd Yunus, M., Shuid, A., Mb, F., Chua, K., Ghafar, N., and Rani, R. (2019). The Effect of Stichopus chloronotus Aqueous Extract on Human Osteoarthritis Articular Chondrocytes in Three-Dimensional Collagen Type I Hydrogel in vitro. *Sains Malaysiana*, **48**, 1671–1683. https://doi.org/10.17576/jsm-2019-4808-13

Mondol, M. A. M., Shin, H. J., Rahman, M. A., and Islam, M. T. (2017). Sea Cucumber Glycosides: Chemical Structures, Producing Species and Important Biological Properties. *Marine Drugs*, **15**(10). https://doi.org/10.3390/md15100317

Moraes, G., Norhcote, P. C., Kalinin, V. I., Avilov, S. A., Silchenko, A. S., Dmitrenok, P. S., Stonik, V. A., and Levin, V. S. (2004). Structure of the major triterpene glycoside from the sea cucumber Stichopus mollis and evidence to reclassify this species into the new genus Australostichopus. *Biochemical Systematics and Ecology*, **32**(7), 637–650. https://doi.org/10.1016/j.bse.2004.02.005

Najmi, A., Javed, S. A., Al Bratty, M., and Alhazmi, H. A. (2022). Modern approaches in the discovery and development of plant-based natural products and their analogues as potential therapeutic agents. *Molecules*, **27**(2), 349. https://doi.org/10.3390/molecules27020349

Nandiyanto, A., Ragadhita, R., Fiandini, M., and Ijost, I. (2023). Interpretation of Fourier Transform Infrared Spectra (FTIR): A Practical Approach in the Polymer/Plastic Thermal Decomposition. *Indonesian Journal of Science and Technology*, **8**, 113–126. https://doi.org/10.17509/ijost.v8i1.53297

Ning, Y.-C. (2011). Interpretation of Infrared Spectra. In *Interpretation of Organic Spectra* (pp. 129–146). https://doi.org/10.1002/9780470825181.ch5

Park, J.-I., Bae, H.-R., Kim, C. G., Stonik, V. A., and Kwak, J.-Y. (2014). Relationships between chemical structures and functions of triterpene glycosides isolated from sea cucumbers. *Frontiers in Chemistry*, **2**. https://doi.org/10.3389/fchem.2014.00077

Pettit, G., Herald, C. L., and Herald, D. L. (1976). Antineoplastic agents XLV: Sea cucumber cytotoxic saponins. *Journal of Pharmaceutical Sciences*, **65**(10), 1558–1559. https://doi.org/10.1002/jps.2600651042

Podolak, I., Galanty, A., and Sobolewska, D. (2010). Saponins as cytotoxic agents: a review. *Phytochemistry Reviews : Proceedings of the Phytochemical Society of Europe*, **9**(3), 425–474. https://doi.org/10.1007/s11101-010-9183-z

Podolak, I., Grabowska, K., Sobolewska, D., Wróbel-Biedrawa, D., Makowska-Wąs, J., and Galanty, A. (2023). Saponins as cytotoxic agents: an update (2010–2021). Part II—Triterpene saponins. *Phytochemistry Reviews*, **22**(1), 113–167. https://doi.org/10.1007/s11101-022-09830-3

Pradhan, B., Bhuyan, P. P., and Ki, J.-S. (2023). Immunomodulatory, Antioxidant, Anticancer, and Pharmacokinetic Activity of Ulvan, a Seaweed-Derived Sulfated Polysaccharide: An Updated Comprehensive Review. *Marine Drugs*, **21**(5). https://doi.org/10.3390/md21050300

Ridzwan, B. H. (2007). Sea cucumbers, a Malaysian heritage. *Research Centre of International Islamic University Malaysia (IIUM), Kuala Lumpur Wilayah Persekutuan: Kuala Lumpur, Malaysia*.

Ridzwan, B. H., Zarina, M. Z., Kaswandi, M. A., Nadirah, M., and Shamsuddin, A. F. (2001). The antinociceptive effects of extracts from Stichopus chloronotus Brandt. *Pakistan Journal of Biological Science*, **4**(3), 244–246.

Riguera, R. (1998). Isolating bioactive compounds from marine organisms. *Oceanographic Literature Review*, **45**(3), 579.

Sanjeewa, K. K. A., and Herath, K. (2023). Bioactive secondary metabolites in sea cucumbers and their potential to use in the functional food industry. *Fisheries and Aquatic Sciences*, **26**(2), 69–86. https://doi.org/10.47853/FAS.2023.e6

Shakoor, R., Hussain, N., Younas, S., and Bilal, M. (2023). Novel strategies for extraction, purification, processing, and stability improvement of bioactive molecules. *Journal of Basic Microbiology*, **63**(3–4), 276–291. https://doi.org/10.1002/jobm.202200401

Shimizu, Y., and Li, B. (2008). *Purification of Water-Soluble Natural Products* (pp. 415–438). https://doi.org/10.1385/1-59259-955-9:415

Silchenko, A. S., Avilov, S. A., Antonov, A. A., Kalinin, V. I., Kalinovsky, A. I., Smirnov, A. V, Riguera, R., and Jiménez, C. (2002). Triterpene glycosides from the deep-water North-Pacific sea cucumber Synallactes nozawai Mitsukuri. *Journal of Natural Products*, **65**(12), 1802–1808. https://doi.org/10.1021/np0202881

Silchenko, A. S., Avilov, S. A., Kalinin, V. I., Kalinovsky, A. I., Dmitrenok, P. S., Fedorov, S. N., Stepanov, V. G., Dong, Z., and Stonik, V. A. (2008). Constituents of the sea cucumber Cucumaria okhotensis. Structures of okhotosides B1-B3 and cytotoxic activities of some glycosides from this species. *Journal of Natural Products*, **71**(3), 351–356. https://doi.org/10.1021/np0705413

Silchenko, A. S., Kalinovsky, A. I., Avilov, S. A., Andrijaschenko, P. V, Popov, R. S., Chingizova, E. A., Kalinin, V. I., and Dmitrenok, P. S. (2021). Triterpene Glycosides from the Far Eastern Sea Cucumber Psolus chitonoides: Chemical Structures and Cytotoxicities of Chitonoidosides E1, F, G, and H. *Marine Drugs*, **19**(12), 696. https://doi.org/10.3390/md19120696

Silchenko, A. S., Kalinovsky, A. I., Avilov, S. A., Andrijaschenko, P. V, Popov, R. S., Dmitrenok, P. S., Chingizova, E. A., and Kalinin, V. I. (2020). Kurilosides A(1), A(2), C(1), D, E and F-Triterpene Glycosides from the Far Eastern Sea Cucumber Thyonidium (= Duasmodactyla) kurilensis (Levin): Structures with Unusual Non-Holostane Aglycones and Cytotoxicities. *Marine Drugs*, **18**(11). https://doi.org/10.3390/md18110551

Silchenko, A. S., Kalinovsky, A. I., Avilov, S. A., Popov, R. S., Chingizova, E. A., Menchinskaya, E. S., Zelepuga, E. A., Tabakmakher, K. M., Stepanov, V. G., and Kalinin, V. I. (2024). The Composition of Triterpene Glycosides in the Sea Cucumber Psolus peronii: Anticancer Activity of the Glycosides against Three Human Breast Cancer Cell Lines and Quantitative Structure–Activity Relationships (QSAR). *Marine Drugs*, **22**(7), 292. https://doi.org/10.3390/md22070292

Simoben, C. V, Babiaka, S. B., Moumbock, A. F. A., Namba-Nzanguim, C. T., Eni, D. B., Medina-Franco, J. L., Günther, S., Ntie-Kang, F., and Sippl, W. (2023). Challenges in natural product-based drug discovery assisted with in silico-based methods. *RSC Advances*, **13**(45), 31578–31594. https://doi.org/10.1039/D3RA06831E

Sobolewska, D., Galanty, A., Grabowska, K., Makowska-Wąs, J., Wróbel-Biedrawa, D., and Podolak, I. (2020). Saponins as cytotoxic agents: an update (2010–2018). Part I—steroidal saponins. *Phytochemistry Reviews*, **19**(1), 139–189. https://doi.org/10.1007/s11101-020-09661-0

Solehin, S. N., Kamarudin, K. R., Akashah, N., Rehan, A. M., Bakar, M. A. L. A., Badrulhisham, N. S., Ab Rahman, N. S., Akma, U. N., Shahdan, F., and

Azman, H. (2021). Species identification and relationship of Sea Cucumber species from Pulau Tinggi and Sedili Kechil, Johor Based on Ossicle Shape. *Journal of Sustainable Natural Resources*, **2**(1), 38–45. https://doi.org/10.30880/jsunr.2021.02.01.006

Son, A., Park, J., Kim, W., Yoon, Y., Lee, S., Ji, J., and Kim, H. (2024). Recent Advances in Omics, Computational Models, and Advanced Screening Methods for Drug Safety and Efficacy. *Toxics*, **12**(11). https://doi.org/10.3390/toxics12110822

SUGAWARA, T., ZAIMA, N., YAMAMOTO, A., SAKAI, S., NOGUCHI, R., and HIRATA, T. (2006). Isolation of Sphingoid Bases of Sea Cucumber Cerebrosides and Their Cytotoxicity against Human Colon Cancer Cells. *Bioscience, Biotechnology, and Biochemistry*, **70**(12), 2906–2912. https://doi.org/10.1271/bbb.60318

Tang, L., Swezey, R. R., Green, C. E., and Mirsalis, J. C. (2022). Enhancement of sensitivity and quantification quality in the LC–MS/MS measurement of large biomolecules with sum of MRM (SMRM). *Analytical and Bioanalytical Chemistry*, **414**(5), 1933–1947. https://doi.org/10.1007/s00216-021-03829-z

Thomford, N. E., Senthebane, D. A., Rowe, A., Munro, D., Seele, P., Maroyi, A., and Dzobo, K. (2018). Natural Products for Drug Discovery in the 21st Century: Innovations for Novel Drug Discovery. *International Journal of Molecular Sciences*, **19**(6), 1578. https://doi.org/10.3390/ijms19061578

Timilsena, Y. P., Phosanam, A., and Stockmann, R. (2023). Perspectives on Saponins: Food Functionality and Applications. *International Journal of Molecular Sciences*, **24**(17). https://doi.org/10.3390/ijms241713538

Torres, M., Parets, S., Fernández-Díaz, J., Beteta-Göbel, R., Rodríguez-Lorca, R., Román, R., Lladó, V., Rosselló, C. A., Fernández-García, P., and Escribá, P. V. (2021). Lipids in Pathophysiology and Development of the Membrane Lipid Therapy: New Bioactive Lipids. *Membranes*, **11**(12). https://doi.org/10.3390/membranes11120919

Uthicke, S., Conand, C., and Benzie, J. (2001). Population genetics of the fissiparous holothurians Stichopus chloronotus and Holothuria atra (Aspidochirotida): a comparison between the Torres Strait and La Réunion. *Marine Biology*, **139**(2), 257–265. https://doi.org/10.1007/s002270100579

Van Dyck, S., Gerbaux, P., and Flammang, P. (2009). Elucidation of molecular diversity and body distribution of saponins in the sea cucumber Holothuria forskali (Echinodermata) by mass spectrometry. *Comparative Biochemistry and Physiology Part B: Biochemistry and Molecular Biology*, **152**(2), 124–134. https://doi.org/10.1016/j.cbpb.2008.10.011

Van Dyck, S., Gerbaux, P., and Flammang, P. (2010). Qualitative and quantitative saponin contents in five sea cucumbers from the Indian ocean. *Marine Drugs*, **8**(1), 173–189. https://doi.org/10.3390/md8010173

Waksmundzka-Hajnos, M., Sherma, J., and Kowalska, T. (2008). Thin Layer Chromatography in Phytochemistry. In *Thin Layer Chromatography in Phytochemistry*. https://doi.org/10.1201/9781420046786

Wang, X., Li, M., Bai, Y., Du, Y., and Duan, S. (2022). Non-holostane and holostane triterpene glycosides from spawn of sea cucumber Apostichopus japonicus selenka. *Journal of Food Composition and Analysis*, **109**, 104492. https://doi.org/10.1016/j.jfca.2022.104492

Wang, Z., Xiong, Y., Peng, Y., Zhang, X., Li, S., Peng, Y., Peng, X., Zhuo, L., and Jiang, W. (2023). Natural product evodiamine-inspired medicinal chemistry: Anticancer activity, structural optimization and structure-activity relationship. *European Journal of Medicinal Chemistry*, **247**, 115031. https://doi.org/10.1016/j.ejmech.2022.115031

Yamada, K., Hamada, A., Kisa, F., Miyamoto, T., and Higuchi, R. (2003). Constituents of Holothuroidea, 13. Structure of Neuritogenic Active Ganglioside Molecular Species from the Sea Cucumber *Stichopus chloronotus*. *Chemical and Pharmaceutical Bulletin*, **51**(1), 46–52. https://doi.org/10.1248/cpb.51.46

Yang, P., Collin, P., Madden, T., Chan, D., Sweeney-Gotsch, B., McConkey, D., and Newman, R. A. (2003). Inhibition of proliferation of PC3 cells by the branched-chain fatty acid, 12-methyltetradecanoic acid, is associated with inhibition of 5-lipoxygenase. *The Prostate*, **55**(4), 281–291. https://doi.org/10.1002/pros.10243

Yang, W.-S., Qi, X.-R., Xu, Q.-Z., Yuan, C.-H., Yi, Y.-H., Tang, H.-F., Shen, L., and Han, H. (2021). A new sulfated triterpene glycoside from the sea cucumber Colochirus quadrangularis, and evaluation of its antifungal, antitumor and immunomodulatory activities. *Bioorganic & Medicinal Chemistry*, **41**, 116188. https://doi.org/10.1016/j.bmc.2021.116188

Yin, H., Li, R., Liu, J., Sun, Y., Zhao, L., Mou, J., and Yang, J. (2024). Fucosylated chondroitin sulfate from sea cucumber Stichopus chloronotus alleviate the intestinal barrier injury and oxidative stress damage in vitro and in vivo. *Carbohydrate Polymers*, **328**, 121722. https://doi.org/10.1016/j.carbpol.2023.121722

Zelepuga, E. A., Silchenko, A. S., Avilov, S. A., and Kalinin, V. I. (2021). Structure-Activity Relationships of Holothuroid's Triterpene Glycosides and Some In Silico Insights Obtained by Molecular Dynamics Study on the Mechanisms of Their Membranolytic Action. *Marine Drugs*, **19**(11). https://doi.org/10.3390/md19110604

Zhang, S.-Y., Yi, Y.-H., and Tang, H.-F. (2006). Bioactive triterpene glycosides from the sea cucumber Holothuria fuscocinerea. *Journal of Natural Products*, **69**(10), 1492–1495. https://doi.org/10.1021/np060106t

Zou, Z.-R., Yi, Y.-H., Wu, H.-M., Wu, J.-H., Liaw, C.-C., and Lee, K.-H. (2003). Intercedensides A-C, three new cytotoxic triterpene glycosides from the sea cucumber Mensamaria intercedens Lampert. *Journal of Natural Products*, **66**(8), 1055–1060. https://doi.org/10.1021/np030064y